CHEMICAL ANALYSIS, BIOLOGICAL ACTIVITIES, AND GREEN SYNTHESIS OF SILVER NANOPARTICLES USING BIOACTIVE *RHUS CHINENSIS* MILL EXTRACTS

A DISSERTATION SUBMITTED FOR THE PARTIAL FULFILLMENT OF THE REQUIREMENT FOR THE MASTER OF SCIENCE DEGREE IN CHEMISTRY

Submitted by

Manisha Bhusal

Exam Roll No.: CHE 1728/076

T.U. Regd No.: 5-2-37-1325-2015

Submitted to

Central Department of Chemistry

Institute of Science and Technology

Tribhuvan University

Kirtipur, Kathmandu

Nepal

June 2023

BOARD OF EXAMINERS AND CERTIFICATE OF APPROVAL

This dissertation entitled **"CHEMICAL ANALYSIS, BIOLOGICAL ACTIVITIES, AND GREEN SYNTHESIS OF SILVER NANOPARTICLES USING BIOACTIVE *RHUS CHINENSIS* MILL EXTRACTS" by** Manisha Bhusal under the supervision of Associate Prof. Dr. Khaga Raj Sharma Central Department of Chemistry, Tribhuvan university, Nepal is here submitted and approved for the partial fulfillment of the Master of Science in Chemistry.

……..

Supervisor

Dr. Khaga Raj Sharma

Central Department of Chemistry

Tribhuvan University

Kirtipur, Kathmandu, Nepal

…….	**…...……**
External Examiner	**Internal Examiner**
Asst.Prof, Dr. Deval Prasad Bhattarai	Prof. Dr. Niranjan Parajuli
Amrit Campus	Central Department of Chemistry
Tribhuvan University Kathmandu, Nepal	Tribhuvan University Kirtipur, Kathmandu, Nepal

……..

Head of Department

Prof. Dr. Jagadeesh Bhattarai

Central Department of Chemistry

Tribhuvan University Kirtipur, Kathmandu, Nepal

Date: July 17, 2023

RECOMMENDATION LETTER

This is to certify that the dissertation work entitled **"CHEMICAL ANALYSIS, BIOLOGICAL ACTIVITIES AND GREEN SYNTHESIS OF SILVER NANOPARTICLES USING BIOACTIVE *RHUS CHINENSIS* MILL EXTRACTS",** has been carried out by "Manisha Bhusal" as the partial fulfillment of the requirement of a Master of Science in Chemistry under my supervision. To the best of my knowledge, the results presented here are her original findings. I hereby, recommend this thesis for the final evaluation.

…….

Supervisor

Dr. Khaga Raj Sharma

Central Department of Chemistry

Tribhuvan University

Kirtipur, Kathmandu,

Nepal

Date:

DECLARATION

I **Manisha Bhusal** hereby declare that the work presented here in genuine work done originally by me and has not been published or submitted elsewhere for the requirement of a degree program. Any literature, data, or works done by others and cited in this dissertation has been given due acknowledgment and listed in the reference section

……..

Manisha Bhusal

bhusalmanisha098@gmail.com

Central Department of Chemistry

Tribhuvan University

Kirtipur, Kathmandu,

Nepal

ACKNOWLEDGEMENT

I would like to express by heartfelt gratitude to my respected supervisor, **Dr. Khaga Raj Sharma**, for his continuous guidance, inspiration, and his excellent suggestion. I am highly grateful for his consistent effort in directing and suggesting throughout the entire research journey.

I would like to express my deep respect and gratitude to **Prof. Dr. Jagadeesh Bhattarai**, Head of the Department for providing an opportunity and platform for conducting this dissertation work in the Central Department of Chemistry and fulfilling all the requirements.

I would like to express my gratitude to my respected **Prof. Dr. Niranjan Parajuli** and the **antibiotics group** for the antimicrobial assay and continuous support during research work and also like to be thankful to Assistant Professor **Ishwor Pathak** sir for supporting me for FE-SEM, EDX, and color mapping during the research activities.

I would also like to acknowledge all the faculty members, to all my professors, technicians, and administrative staff for making me more comfort during my dissertation work. Similarly, I would also like to be thankful to the **National Herbarium and Plant Laboratories**, Godavari for the identification of plants, and the **National Academy of science and technology Khumaltar (NAST)**, Lalitpur for XRD analysis as well as for providing grant which made me more financial support during my research journey.

I would like to express my deep gratitude to my beloved family for their endless support, love, and encouragement. Without them, I would not be the person I am today. My special thanks to my Natural Product team or Nano mates **Kamana Sharma, Anita Bhadel, Jyoti Subedi, Jyoti Pant, Saraswoti Karn, and Ravi Bhusan Sharma** for their help and company during this dissertation work.

Thank you all

Manisha Bhusal

bhusalmanisha098@gmail.com

ABSTRACT

Rhus chinensis is a tiny deciduous perennial shrub in which its leaves, roots, and fruits parts are being used to cure depurative, costimulatory blood circulation, hemoptysis, inflammations, laryngitis, traumatic fractures, snake bite, colic, diarrhea, dysentery, jaundice, and hepatitis. This study aimed to estimate the total phenolic content, total flavonoid content, and antibacterial and antioxidant activities of *Rhus chinensis* extracts and semi-purified fractions of different parts and also to undertake the green synthesis of silver nanoparticles utilizing *Rhus chinensis* plant extract in an ecofriendly, cost-effective, and more efficient manner with its antimicrobial application. The total phenolic content and total flavonoid content in *Rhus chinensis* were found to be 141.480 ±0.665 mg GAE/g in methanolic extract of root and 54.345 ±0.279 mg QE/g in ethyl acetate extract of root. DPPH radical scavenging activity showed the crude extract of *Rhus chinensis* root was found potent of inhibitory concentration (IC_{50}) 7.830 ±0.187 µg/mL as compared to the standard quercetin (IC_{50}) value 2.2567± 0.296 µg/mL. *Rhus chinensis* root was found active against ATCC 43300 *Staphylococcus aureus* of ZOI 22 mm whereas, ZOI of positive control Neomycin was found to be 25mm. *Rhus chinensis* leaf extract was found effective against ATCC 25922 *Escherichia coli* of ZOI 25 mm, respectively and ZOI of positive control Neomycin for these bacteria was found to be 20 mm. Color change from yellowish to reddish brown can be visualized which indicated the presence of silver nanoparticles. The UV-vis absorption peak of synthesized AgNPs root and leaf extract was found at 443nm and 441nm respectively. The functional group may act as capping and stabilizing agents, as evidenced by the functional group's moving position in the FTIR spectra. The crystallites size of synthesized AgNPs of RC- root and RC-leaf was found to be 11.01 nm and 13.39 nm respectively, while with the help of SEM image the shape and particle size of synthesized AgNPs root and leaf extract was relatively found to be spherical with a diameter of 54.40nm and 30.89 nm respectively. The presence of an intense silver component was confirmed by EDX analysis. Both synthesized AgNPs showed higher zones of inhibition (ZOI) on the disk-diffusion method against both Gram-positive and Gram- negative bacteria.

Keywords: *Rhus chinensis*, biological activities, antioxidant, antimicrobial, green synthesis, silver nanoparticles. DPPH, ZOI.

TABLE OF CONTENTS

LIST OF TABLES

LIST OF FIGURES

LIST OF ABBREVIATIONS

DMSO	Dimethyl sulphoxide
DCM	Dichloromethane
DPPH	2, 2 –diphenyl-1-picrylhydrazyl
FCR	Folin Ciocalte reagent
FTIR	Fourier transfer infrared spectroscopy
EDX	Energy-dispersive X-ray spectroscopy
FE-SEM	Field emission- scanning electron spectroscopy
g/L	Gram per liter
GAE	Gallic acid equivalent
IC50	Half minimal inhibitory concentration
LSPR	Localized surface Plasmon resonance
µg/mL	Micro gram per milliliter mg
QE/g	Milligram quercetin equivalent per gram
MHA	Muller Hilton agar
nn	Nanometer
RC	*Rhus chinensis*
RNS	Reactive nitrogen species
ROS	Reactive oxygen species
TPC	Total phenolic content
UV	Ultra violet
XRD	X-ray diffraction
ZOI	Zone of inhibition

CHAPTER-1

INTRODUCTION

1.1 General introduction

Nepal is abundant in medicinal herbs, wildlife, and socio-cultural biodiversity. In Nepal, numerous substances from plants are utilized in traditional medicine for the treatment of either chronic or infectious disorders (Alam & Sharma, 2020). Plants and plant products have been used as the main stage of everyday life by voluminous people since the dawn of human civilization. Secondary metabolites such as saponin, flavonoids, alkaloids, tannins, lipids, carbohydrates, etc. are found in medicinal plants which are a possible source of curative therapeutics, with a broad list of compounds that have therapeutic potential. Nepal is a small landlocked and hilly country that stretches from 26° 22′ to 30° 27′ N and 80°04′ to 88° 12′ E, covering an area of 147,181 km^2 (Karki et al., 2016). Indicators of development collected by the World Bank and derived from authorized sources show that Nepal's forest area, which is a percentage of the land area, was recorded at 41.59 percent in 2020.

The district Arghakhanchi, which is part of Nepal's Western Development Region, is located between 270 45' and 280 06' N latitude and 800 54'-830 23' E longitude, covering 1193 square kilometers (Panthi & Singh, 2013). The Mahabharata Range covers 68 % of the area, while the Siwalik Hills cover the rest. The elevation ranges from 305 to 2575 meters above sea level, and around 40% of the land is forested. This district is rich in ethno medicinal plants and several species of plants are found which are used as medicine to treat several diseases such as fever, dysentery, diarrhea, body pain, sugar, blood pressure, etc. Medicinal plants have proven to be invaluable in world health, both in terms of maintaining health and in the development of new treatments. The World Health Organization, or WHO reports that conventional medicine is the major method of health care for roughly 80% of the population in impoverished countries (Acharya, 2012).

The medicinal herbs are used by the majority of Nepalese people against simple to life-threatening diseases. In Nepal's livelihood, health, and socioeconomic prospects, medicinal and aromatic plants play a crucial role (Sharma et al., 2015). This study carried out the whole parts such as fruit, leaves, root, and bark of *Rhus Chinensis*

(Bhakiamlo) which was collected from the Chhatradev rural municipality of the western part of Arghakhanchi district. The majority of people have been using *Rhus chinensis* plant parts as medicine against various diseases, for food, fodder, etc. Its fruit part is used for producing natural vinegar and spice, usually sour (Zhang, Ma, Gao, et al., 2018). *Rhus chinensis* Mill is a tiny deciduous perennial shrub or tree in the Anacardiaceae family containing more than 200 individual species which is found in temperate and tropical regions worldwide (Shi et al., 2019). It is commonly called Chinese sumac, Chinese gall, or nutgall tree. Folk medicine physicians in Asia have traditionally employed *Rhus chinensis*. It blooms with white flowers in August or September and bears fruit in October. Red, globose somewhat flattened drupes with one seed are the mature fruits of this shrub (Wu et al., 2018). *Rhus chinensis* is tolerant of a variety of soil types and it's frequently found in areas of uncultivated land (Ren et al., 2008). This study focused on analyzing total phenolic and flavonoid content, antibacterial, anti-oxidant inhibitory activity, extracted using various solvents from whole parts of *Rhus chinensis* (Bhakiamlo), and two different *Rhus chinensis* parts such as leaves, and roots used to create silver nanoparticles which were followed by the standard protocols.

1.1.1 Scientific Classification of Plant

Kingdom: Plantae

Class: Angiosperm

Family: Anacardiaceae

Genus: *Rhus*

Species: *R. chinensis*

Common name: Bhakiamlo

Voucher code number**:** MB-001 (KATH)

Figure 1: *Rhus chinensis* plant

1.2 Phytoconstituents

Phytoconstituents are non-nutrient active plant chemical composition or bioactive chemicals, which are in charge of defending the plant against microbial infections pest infestations, pathogen attacks, and predator attacks. The key phytochemical categories with the greatest structure diversity are phenols, alkaloids, carbohydrates, lipids,

terpenoids, and other nitrogen-containing compounds. In plants, phytochemicals like alkaloids, flavonoids, saponins, polyphenols volatile oil, quinine, carbohydrates, proteins, and so on are found. Phytochemicals can also be divided into several subclasses based on variations in their biogenesis or biosynthetic pathways (Barani et al., 2021). Metabolites are intermediate end products of metabolism. Metabolites are of two types that are primary and secondary. Primary metabolites are crucial for plants' healthy growth and development whereas secondary metabolites are those compounds that are produced by plants for a variety of purposes, including defense. Biological processes including antioxidant, antibacterial, anti-diabetic, anti-inflammatory, antiulcer, and other phytochemical compounds play a vital role (Chhetri et al., 2020). To conduct the phytochemical study, chemicals from the original plant can be first extracted and isolated, and then their structure or composition can be determined. Using lab model systems, such as cultures of cells, research in vitro, or in vivo trials using creatures from the lab to analyze them. A challenge in that area is identifying the phytochemical that is primarily responsible for the given biological effect, as well as separating particular chemicals and figuring out their structures, both are typically challenging (Jones & Kinghorn, 2012).

The plant produces polyphenols as secondary metabolites, and these compounds are frequently used by pathogens to aggregate or as a form of defense against ultraviolet light. The majority of the antioxidant activity in plants and plant products is caused by the biggest group of phytochemicals, known as phenolic. Around 8000 plants phenolic are present in nature. Due to their polyphenolic makeup, they can scavenge dangerous free radicals like superoxides and hydroxyl radicles (Sulaiman & Balachandran, 2012). The presence of polyphenols is reported to be the major secondary metabolite responsible for antioxidant activity. The primary cause of phenolic antioxidant activity is their redox ability to function as metal chelators, oxygen quenchers, hydrogen donors, and reducing agents. The amount of the hydroxyl group in the sample directly correlates to the antioxidant activity of phenolic compounds and flavonoids (Ghasemzadeh et al., 2010).

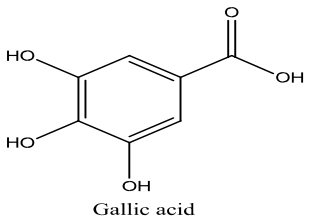

Gallic acid

Flavonoids are polyphenols with at least two phenolic rings, and they can be split into several subclasses, including isoflavones, flavonols, dihydro flavonols, flavan-3-ols, and flavones, (Molyneux et al., 2007). The most prevalent class of polyphenolic chemicals found in plants are flavonoids. Flavonoids are considered strong antioxidants. Flavonoids' active groups of hydroxyl control their antioxidant effects and benefits by neutralizing free radicals and possess defensive properties against numerous pathogenic and deteriorating conditions including cardiovascular diseases, malignancies, and other age-related diseases (Miksicek, 1993). Quercetin, the most well-known flavonoid present in higher plants, exhibits biological actions such as anti-inflammatory, anti-bacterial, anti-viral, and anti-hepatotoxic properties while also inhibiting a variety of enzymes (Muflihah et al., 2021)

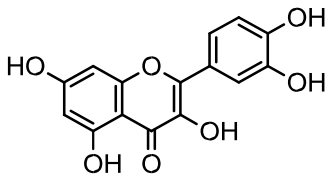

Quercetin

1.3 Antioxidant

Antioxidants are chemicals, either natural or artificial, that may stop or delay oxidative cell damage. An essential component of life is oxygen. Free radicles are produced when oxygen is used by cells to produce energy, as a result of the mitochondria's creation of ATP (adenosine triphosphate). These by-products are often reactive oxygen and nitrogen species (ROS) and reactive nitrogen species (RNS) that come from the cellular redox process (Huy et al., 2008). Antioxidants prevent cell and tissue damage by acting as scavengers. Antioxidants are thought to function in two distinct ways. The chain-breaking process is the first mechanism in which, the primary antioxidant helps the free radical by giving it an electron. The second step is to neutralize the catalyst that starts the chain, which gets rid of the ROS initiators donates an electron to the already existing free radical. The second step involves neutralizing the chain-starting catalyst, which eliminates the ROS initiators (secondary antioxidants) (Sharifi-Rad et al., 2020). Regular consumption of antioxidants can help the body get rid of the free radicals that are already present, improving health by lowering the possibility of developing non-communicable diseases including kidney diseases, cancer, diabetes, cataracts, renal toxicity, and coronary heart diseases. Additionally, antioxidants help shield the skin

from sun-induced edema. Wrinkles UV- induced skin cancer, and skin dryness (Ayoka et al., 2022).

DPPH (2, 2-diphenyl-1-picrylhydrazyl) is frequently employed in vitro techniques to assess radical scavenging capacity. They are synthetic radicals that cannot reproduce in vivo, but they offer a quick, easy, and low-cost way to assess antioxidant efficiency. DPPH (2, 2 -diphenyl-1-picrylhydrazyl) is a persistent organic nitrogen radicle with a rich purple color with a maximal absorbance in the 515-520 nm range. Antioxidants are believed to affect DPPH because of their capacity to donate hydrogen. To stop free radicals from performing their harmful role, radical scavenging actions are crucial. A reliable method for evaluating a plant extract's antioxidant capacity is the DPPH free radical scavenging process. In the DPPH test, the extract is utilized to transform a violet DPPH solution into a yellow chemical, diphenyl picryl hydrazine, in a concentration-dependent manner. This method has been utilized frequently to forecast antioxidant activities because of the short study required (Locatelli et al., 2009), (Rahman et al., 2015)).

1.3.1 Mechanism of Antioxidant

The suggested method entails the addition of a hydrogen atom to the DPPH molecules from an antioxidant to create stable DPPH-H molecules. Ascorbic acid, cysteine, gallic acid, quercetin, vitamin C, vitamin E, selenium, and others are a few examples of antioxidants. By contrasting a plant extract or its constituent with a standard antioxidant, the antioxidant activity of the substance can be ascertained. And in a laboratory, quercetin, ascorbic acid is frequently used as an antioxidant.

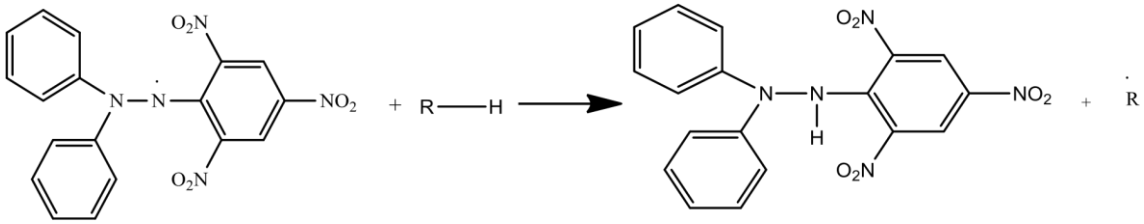

Figure 2: Mechanism of DPPH radical scavenging

1.3.2 Mechanism of quercetin with DPPH

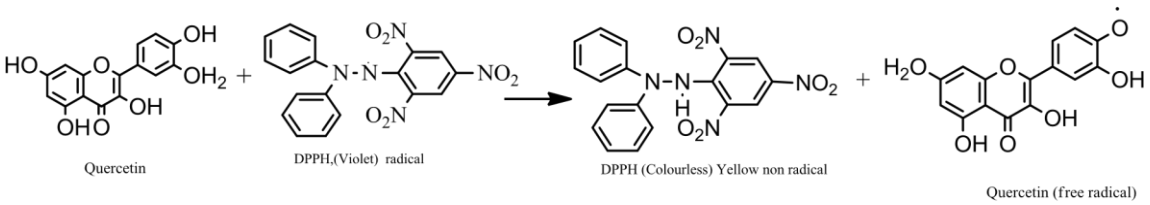

1.4 Antimicrobial activity

The most trustworthy sources for obtaining a range of medicines would be medicinal plants. Numerous medicinal plants have been identified as important sources of naturally occurring antimicrobial chemicals as potential substituents that may be successful in the treatment of these troublesome bacterial illnesses (Iwu et al., 1999). An extract's or a compound's in vitro antimicrobial activity can be assessed or screened using a range of qualitative and quantitative laboratory techniques. Agar well- method and disc-diffusion methods are used to determine antimicrobial activity. The body will experience more side effects from frequent usage of synthetic pharmaceuticals and excessive unneeded medication, and occasionally the poisonous side effects brought on by the use of drugs are much more of a problem. It is, therefore, more important than ever to look for newer antibiotic sources due to the increase in multidrug resistance among pathogenic bacteria (Nieto et al., 2018).

1.5 Nanomaterials

Nanotechnology is the process of creating particles that are in the nanometer range, or between 1 to 100 nm. This range is the nanoscale range. Nanotechnology is the field of study and application of nanostructured particles for industrial purposes. The field of research known as nanotechnology is still in its infancy, but it has the potential to replace conventional technologies and provide useful materials with size-dependent features. Due to their extensive biological and physiochemical applications, many forms of manufactured metal nanoparticles have drawn significant attention worldwide. When nanomaterials are created with the appropriate size, morphology, crystallinity, form, size, and chemical composition, completely new and improved properties are feasible. Because of the large surface area to volume proportion, they exhibit optical quantities since they are small enough to contain their electrons and induce quantum effects, making it simple to detect (Rautela et al., 2019). To address these issues, nanotechnology has attracted a lot of interest. CuO, ZnO, NiO, MnO, and

other metal oxide nanomaterials have applications as, targeted drug delivery systems, antibacterial agents, antimycotic agents, anticancer agents, and antioxidant agents (Khan et al., 2020). Due to their many potential uses in medical devices, silver nanoparticles (AgNPs) are used in extensive research. The applications of nanomaterials in biomedicine, bioimaging, photovoltaics, biomedicine, drug delivery, solar cells, bio labeling, photocatalysis, and data storage, are within the promising options (Melkamu & Bitew, 2021).

Nanomaterials are classified into many groups based on their dimensional like zero-dimensional nanomaterial (nanorods, nanospheres, quantum dots, and nanoclusters, -dimensional nanomaterial (nanotubes, nanowires), two-dimensional nanomaterial (nanosheets, nanofilms), and three-dimensional nanomaterial (bulk materials). Nanoparticles are zero-dimensional nanomaterials. Nanoparticles are present widely in nature and are the objects of study in various fields of science. The top-down strategy and the bottom-up approach are the two main strategies for synthesizing nanomaterials. The top-down method entails using machining, coating, atomization, lithography, and etching processes to reduce bulk materials into nanoparticle size. Building materials up from the bottom up approaches molecules by molecule, atom by atom, or cluster by cluster- is known as the bottom-up method.

1.6 Silver nanoparticles (AgNPs)

Silver nanoparticles are nanoparticles of silver with which sizes ranging from 1 nm to 100 nm. Silver nanoparticles are being used more often in a wide range of sectors because of their unique physical and chemical properties. Comprising health care, pharmaceuticals, and consumer products. Biological characterization is among them powerful optical, electrical thermal, and conductivity characteristics (Zhang et al., 2016). AgNPs are now frequently employed in many different textiles and keyboards, wound dressing, and health care equipment. Due to the uniqueness of nanosized metallic particles and their ability to significantly alter physical. These nanoparticles have been employed for several purposes due to their ratio of surface to volume and chemical and biological capabilities. (Li et al., 2010). There are many different types of nanoparticles, but silver nanoparticles are well-known for their high conductivity, chemical durability, localized surface plasmon resonance, and catalytic properties.

These metal NPs have been prepared using many different methods. These include biological (plants, fungi, bacteria, viruses, yeast, etc.), physical (laser ablation, arc discharge, photolithography, ball milling, etc.), Chemical (Solvothermal, sol-gel, co-precipitation, pyrolysis, etc), technique. Many times, toxic chemicals and solvents are used in physical and chemical processes. Which could hurt the environment (Ahmad et al., 2019). Within the several synthetic techniques for silver nanoparticles. Biological methods seem to be simple, efficient, and harmless. For translational studies, reliable and environmentally friendly methods that can produce well-defined sizes and shapes are best. Finally, a green chemical approach for the synthesis of AgNPs is quite promising (Zhang et al., 2016). In the fields of antifungal, antibacterial, cosmetics, anti-inflammatory, antiviral, anticancer, and more green-produced AgNPs have a wide range of uses (Hussein & Abdullah, 2020).

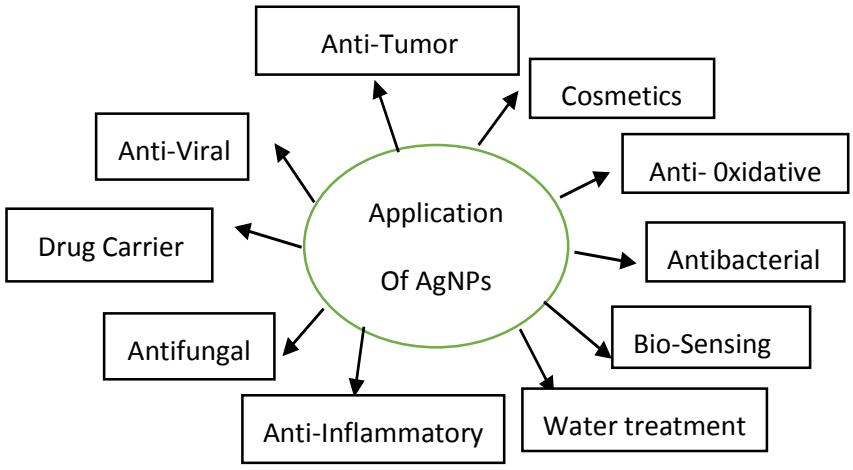

Figure 3: Application of silver nanoparticles

1.7 Mechanism of silver nanoparticles

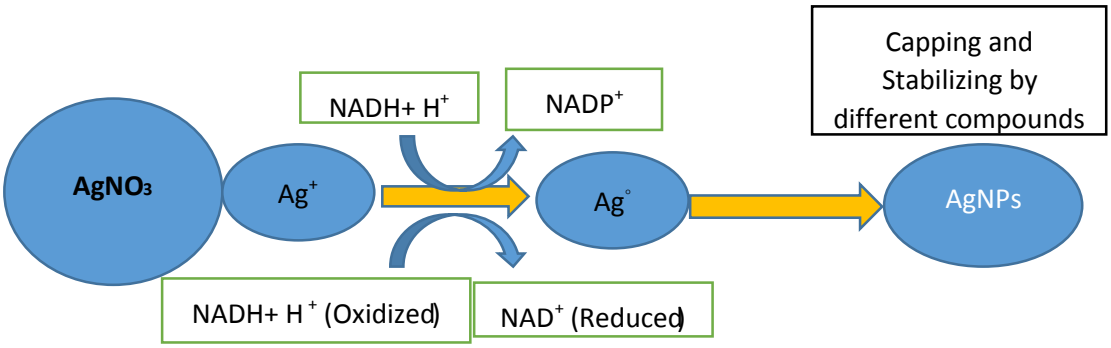

Figure 4: Mechanism of silver nanoparticle synthesis (Mikhailova, 2020).

1.8 Characterization of silver nanoparticles

Silver nanoparticles are generally characterized by using different techniques. Such techniques are Ultraviolet-visible spectroscopy (UV-Vis), Fourier transfer infrared ray (FTIR), X-ray diffraction spectroscopy (XRD), Field emission-scanning electron microscopy (FE-SEM), and Energy Dispersive X-ray (EDX). Other common techniques generally used for characterization they are Zeta potential method,

Localized surface Plasmon resonance (LSPR), Transmission electron microscopy (TEM), X-ray photoelectron spectroscopy (XPS), etc.

1.8.1 UV-visible spectroscopy

UV-Vis spectroscopy is one of the widely used and easiest techniques to confirm the formation of nanoparticles. The absorbance spectrum of different samples is obtained between 200 to 800 nm, and double distilled water is used as a reference solvent to adjust the baseline. (Anandalakshmi et al., 2016). It is one of the preliminary methods for the characterization of silver nanoparticles which helps to check out the stability of silver nanoparticles. Temperature, pH, pressure, time, particle size, pore size, and environment greatly influence the stability of synthesized nanoparticles. After diluting the sample many times with distilled water, the UV-Visible spectra of solutions were measured to track the reduction of silver ions to nanoparticle form (Ashraf et al., 2016). These methods required a short time of measurement. Silver nanoparticles conduction and valence bands are close to one another, which allows electrons to flow freely to produce the local surface Plasmon resonance band as a result of collective oscillation (Link & El-Sayed, 2003). The wavelength with the greatest absorption is referred to as the maximum value and its value range from 400 to 450nm.

1.8.2 Fourier transfer infrared spectroscopy (FTIR)

Fourier transfer infrared spectroscopy is one of the widely used characterization techniques to detect the possible functional groups in biomolecules present in the plant sample. The analysis of the bonding structures produced by interactions between metal particles and biomolecules is done by FTIR (Periasamy et al., 2022). With the use of several phytochemicals, the FTIR was used to analyze the conversion of inorganic silver nitrate to silver. These phytochemicals are employed as aping agents, stabilizers, and reductants (Arshad et al., 2018). The frequency range for absorption is between

400 and 4000 cm^{-1}. The computer's software uses spectrum data to identify exact groups.

1.8.3 X-ray diffraction (XRD)

X-ray diffraction is a useful characterization technique to calculate the size of crystalline nanoparticles, determine the crystal structure, and demonstrate the creation of AgNPs. The presence of silver nanoparticles in plant tissue can be detected by utilizing XRD to analyze the diffraction peaks of the AgNPs, which is a standard method for evaluating the material's crystal structure and chemical structure (A & S, 2018). XRD is utilized for the measurement of mineralogical data as well as the qualitative identification of minerals in geological samples using fingerprinting approach (Al-Jaroudi et al., 2007).

1.8.4 Field emission- scanning electron microscopy (FE-SEM)

Field emission-scanning electron microscopy is one of the important characterization techniques that gives information about the size shape, and morphology of the samples, shape, and size. It is capable of exploring the surface morphology of nanoparticles because it detects scattered electrons from the particle's surface and is also used to determine the particle size of silver nanoparticles. FE-SEM has the drawback of being unable to resolve interior structure, but it is still capable of giving useful information on purity and particle aggregation levels. The morphology of nanoparticles less than 10 nm can be determined using a current high-resolution FE-SEM (Zhang et al., 2016).

1.8.5 Energy-dispersive X-ray spectroscopy (EDX)

Energy dispersive X-ray (EDX) is one of the most important and easiest techniques which are used for the identification of the element composition of a specimen (Zheng et al., 2011). Spot detection analysis of regions up to 10 cm in diameter, contaminant identification, material evaluation and identification, quality control screening, and other processes are applications of EDX.

1.9 Thin layer chromatography (TLC)

TLC is a preliminary test that is frequently used for sample screening before utilizing confirmatory procedures and in an environment with limited resources (Mwankuna et

al., 2023). Because of its simplicity, low cost, high sensitivity, and speed of separation, it is widely used. TLC is used for purity tests and also for the isolation of compounds.

If the sample is pure, a single spot is seen.

1.10 Objectives

1.10.1 General objective

The general objective of this research was the analysis of secondary metabolites that leads to the biological activity of various solvent extracts and the synthesis of silver nanoparticles of *Rhus chinensis* Mill growing in the Chhatradev rural municipality of Arghakhanchi district.

1.10.2 Specific objective

- Performance of preliminary phytochemical screening of the plant extracts.
- Estimation of the total phenolic and flavonoid content.
- Study of the antibacterial and antioxidant properties of different plant extracts.
- Synthesis of silver nanoparticles using plant extracts and their characterization.
- Study of antibacterial activity of green synthesized silver nanoparticles

CHAPTER-2

LITERATURE REVIEW

The information included in the literature review of the research on the chosen plant, *Rhus chinensis*, was discussed in order of appearance in books, journal papers (Scholarly articles), and websites (Sci-hub, Google, Google Scholar).

Shi et al., 2019 isolated the protein content of *Rhus chinensis* Mill seeds was relatively high (14.38 1.24- 14.88 0.85 %), While the oil in the fruits was relatively high (19.68

0.68-20.27 1.33%), it was rich in linoleic acid and other unsaturated fatty acids (51.41 1.18-53.76 3.01% and 74.82 3.14-75.58 2.32%, respectively). Its seed oils had much better antioxidant capabilities than the fruit oils because of their high amount of tocopherol/ tocotrienol, polyphenol, and phytosterol.

Zhang et al., 2018 investigated *Rhus chinensis* the predominant phenolics in all fractions were myricitrin and quercetin, which displayed good dose-dependent lipase inhibitory effects, with myricitrin having a larger inhibitory impact. Myricitrin attaches more securely to the lipase than quercetin with more hydrogen bonds and a shorter distance between them, indicating that myricitrin had lipase inhibitory activity and correlating with their experimental findings.

Djakpo & Yao, 2010 found that in –vitro chemicals from the stem of *Rhus chinensis* reduced HIV-1 activity, inhibited enamel demineralization, and improved fluoride remineralization of dental enamel, and improved fluoride remineralization of dental enamel.

Zhang, Ma, Zhao, et al., 2018 investigated *R. chinensis* Mill fruit extracts extracted with 80% ethanol and 80% acetone were found to have the highest phenolic levels, and 13 of 14 known phytochemical constituents were phenolic compounds quercetin-3-Orhamnoside and Myricetin-3-O-rhamnoside were the two phenolics that were present in all of the extracts most frequently. The high antioxidant and pancreatic lipase inhibitory activity of the three extracts has been shown in vitro.

Dhakal et al., 2022 examined *R. chinensis* fruit had a total of 62.41 mg QE/g and 117.092 mg GAE/g of phenols and flavonoids, respectively. The antioxidant activity of the crude extract and its fractions had an IC_{50} value that ranged from 3.12115 µg/mL

to 50.852.10 µg/mL. *Staphylococcus aureus* with a ZOI value of 11 mm and *Bacillus subtilis* with a ZOI value of 9.0 mm were two gram-positive bacteria that *R. chinensis* was successful against.

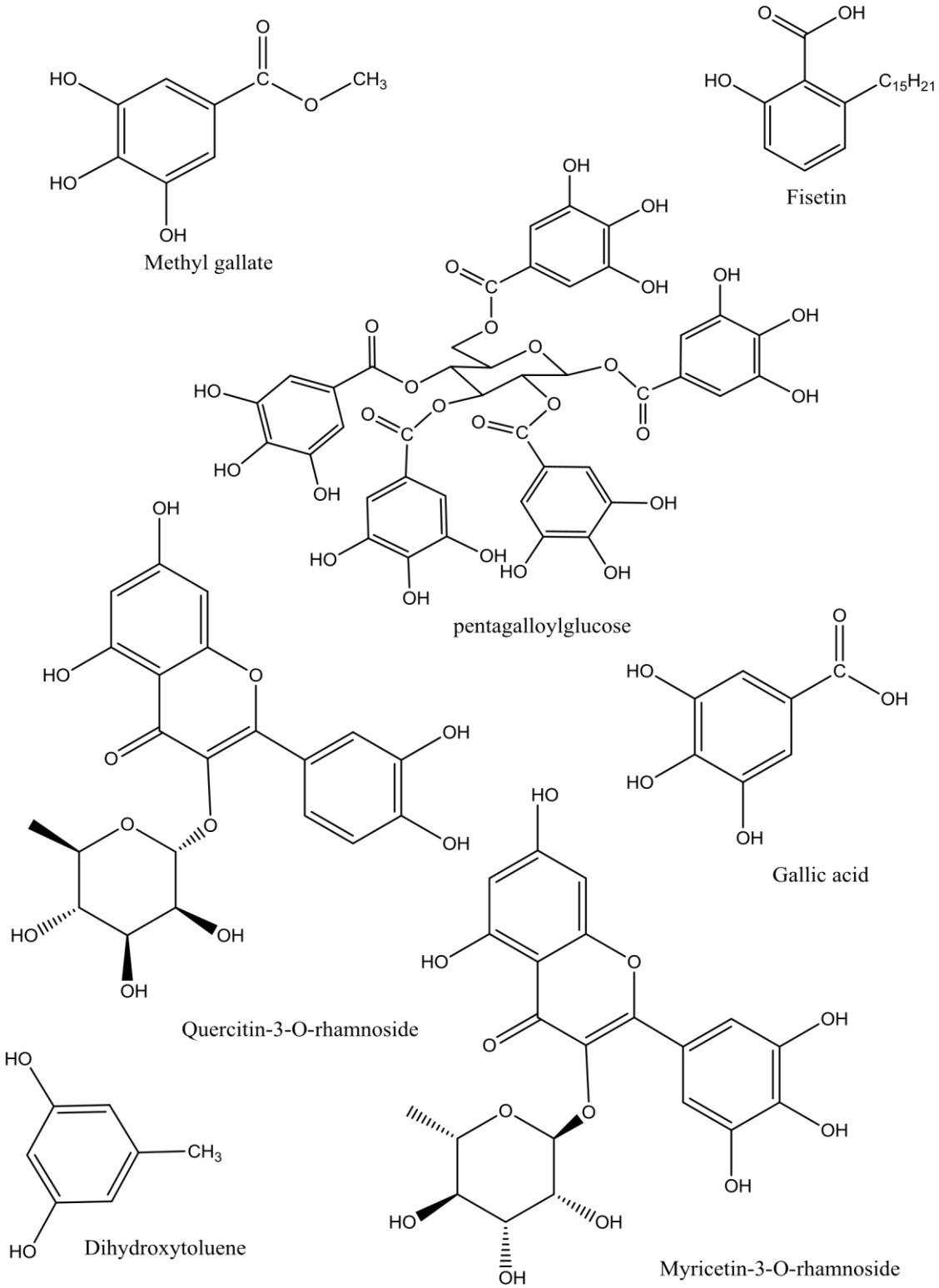

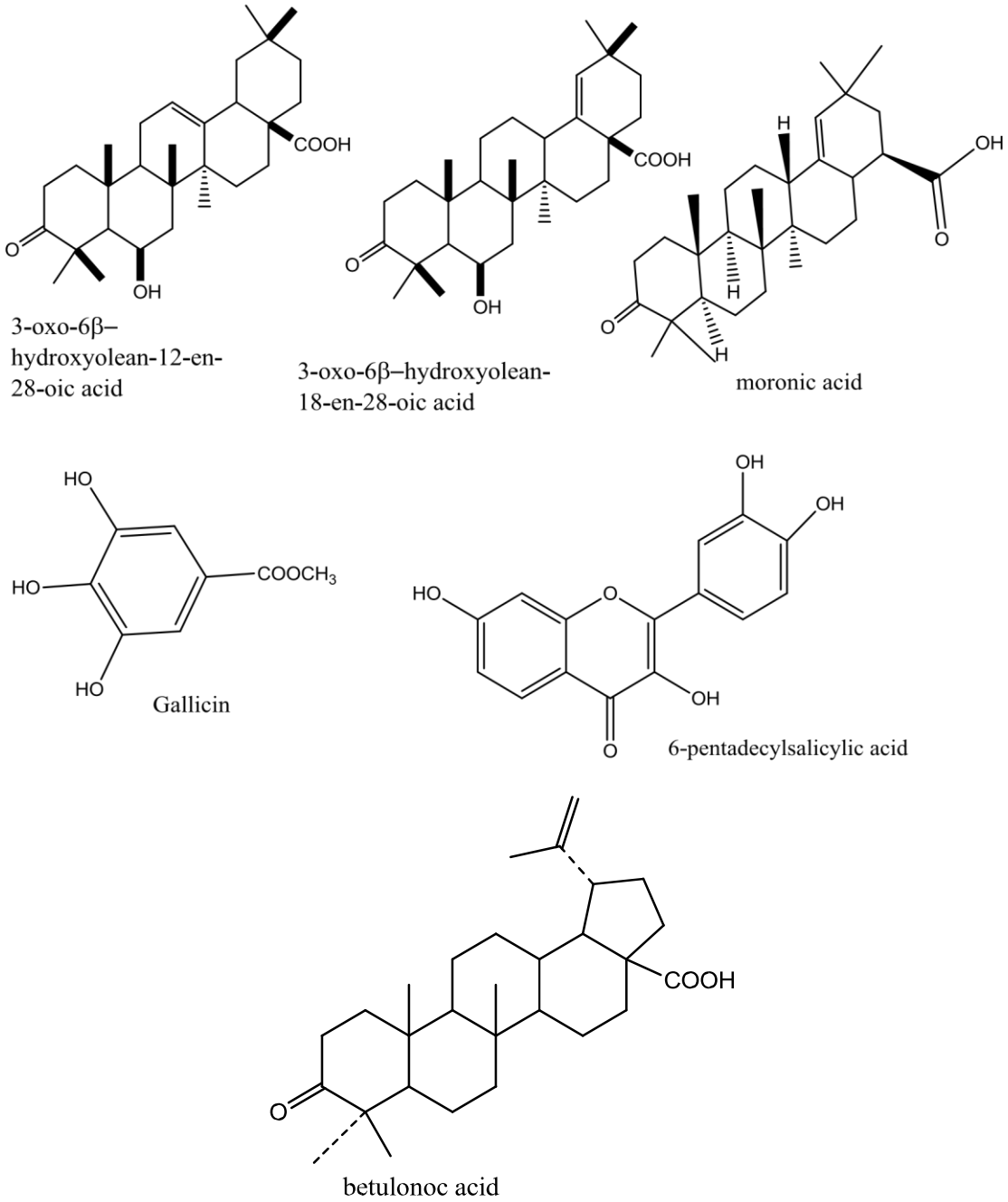

Figure 5: Structures of selected bioactive compound from plant *Rhus chinensis* Mill

Tian et al., 2009 found that the gall-tannins of galla chinensis were successively extracted by five solvents of various polarity, as a result of their increased molecular weight and stronger antioxidant and antibacterial properties, the extracts with less polarity were found to include gall-tannins.

Sariozlu & Kivanc, 2011 investigated gallnuts have promised future use in human health as a food supplement, antioxidant, antibacterial agent, diabetic therapy, in the

dermatology and pharmaceutical industries, as an anti-pigment agent in the cosmetic sector, or as a natural pesticide, among other things.

Patil et al., 2016 investigated synthesized AgNPs of the gall of *Rhus chinensis* were found to be 150 nm in size and have triangular, oval, and hexagonal geometries. An absorption peak was found around 450 nm which was reported by UV-Visible spectroscopy whereas FTIR analysis reported the presence of functional groups such as C–C, C–O, C–O–C, =C–H, and C=O in AgNPs synthesis.

CHAPTER-3

MATERIALS AND METHODS

3.1 Materials required

3.1.1 Equipment and Apparatus

Beaker, volumetric flask, conical flask, measuring cylinders, test tubes, funnel, glass wares, aluminum foil, filter papers, reagent bottles, and pipettes were used for this work. All the glass wares were manufactured from class 1 borosilicate glass from Borosil Company.

Grinding mill, rotatory evaporator, weighing balance, water bath(Clifton), 96 well plates, magnet, magnetic stirrer (Nike), pH-meter (Deluxe), plastic vials, incubator, UV spectrophotometer (SPECORD 200 PLUS, (An Endress+Hauser Company), IRT racer100 (Fourier transform infrared spectrophotometer), desiccator, dropper, centrifuge tube, centrifuge instrument (Sorvall ST 8R), Microplate reader (Epoch 2, Biotek, Instruments, Inc, USA) and Petri-plate were used during this work.

3.1.2 Chemicals

All the chemicals and solvents were used in analytical-grade laboratories. Some organic solvents like methanol (CH_3OH, Fischer Scientific), ethyl acetate, dichloromethane (DCM), hexane (Merck), ethanol, dimethyl sulphoxide (DMSO), sodium carbonate (Na_2CO_3), FC-reagent (FCR), quercetin, gallic acid 2,2-diphenyl-1-picrylhydrazyl (DPPH), aluminum chloride ($AlCl_3$), sodium hydroxide (NaOH), silver nitrate ($AgNO_3$), Muller Hinton Agar (MHA) and sodium acetate were available in lab. All the chemicals were from Merck and Sigma Company.

3.2 Plant sample collection and Identification

The different parts such as leaves, fruit, bark, and root of the plant *Rhus chinensis* were collected from western Nepal, Arghakhanchi district. The plant parts collected were in their wild and natural habitat. The plant was identified by the locals as a medicinally valuable plant. The collected area is Chhatradev-4 Rural Municipality, Arghakhanchi district, Province No. 5, Lumbini. It is situated at an altitude of 2515 m with latitude 28′45′′N and longitude 83′23′′E. The plant was collected in June and July 2022. After the collection of the plant, its herbarium was prepared the plant was identified by a

taxonomist from Godawari Lalitpur's National Herbarium and Plant Laboratories. Nepal as *Rhus chinensis* Mill of family Anacardiaceae with voucher code no. MB-OO1 (KATH).

3.2.1 Preparation of plant extract

Different parts of plant materials were thoroughly washed with clean water and cut into smaller pieces and dried in a shaded place where there is no presence of sunlight for two weeks and then ground into powder form with the help of a mechanical grinder. The powdered form of the sample was collected in separate tagged waterproof zip-locked plastic bags. The storage and prevention of the sample from external contamination from air and water were highly taken into consideration.

The extract of the powdered plant materials was produced using various solvents like distilled water, methanol, ethyl acetate, DCM, and hexane based on polarity by using cold percolation methods. 50 g of powdered leaves sample, 40 g of powdered root sample and 22 g of bark sample, and 50 g of fruit sample were soaked in different five solvents on a ratio of 1: 10 ratio in a 1000 mL conical flask for 72 hours. The solution was shaken every 24 hours with continuous agitation. After completion then the solution was filtered through Whatman filter paper. Thus, obtained filtrate was a different extract of the plant sample. The process was repeated three times.

3.2.2 Concentration of the extract

The prepared different solvent extracts were concentrated by using a rotary evaporator maintaining the temperature at 40℃ and pressure of about 650 mmHg. The obtained concentrate from the rotatory evaporator was then kept in a water bath for the complete removal of the solvent to obtain the viscous mass of crude extract. After that then the crude extracts were stored in a borosilicate glass tube to check their phytochemical analysis and biological activities at low temperatures.

Percentage yield = Dry weight of extracts / Dry weight of plant materials ×100

The schematic diagram for showing the methodology of the research:

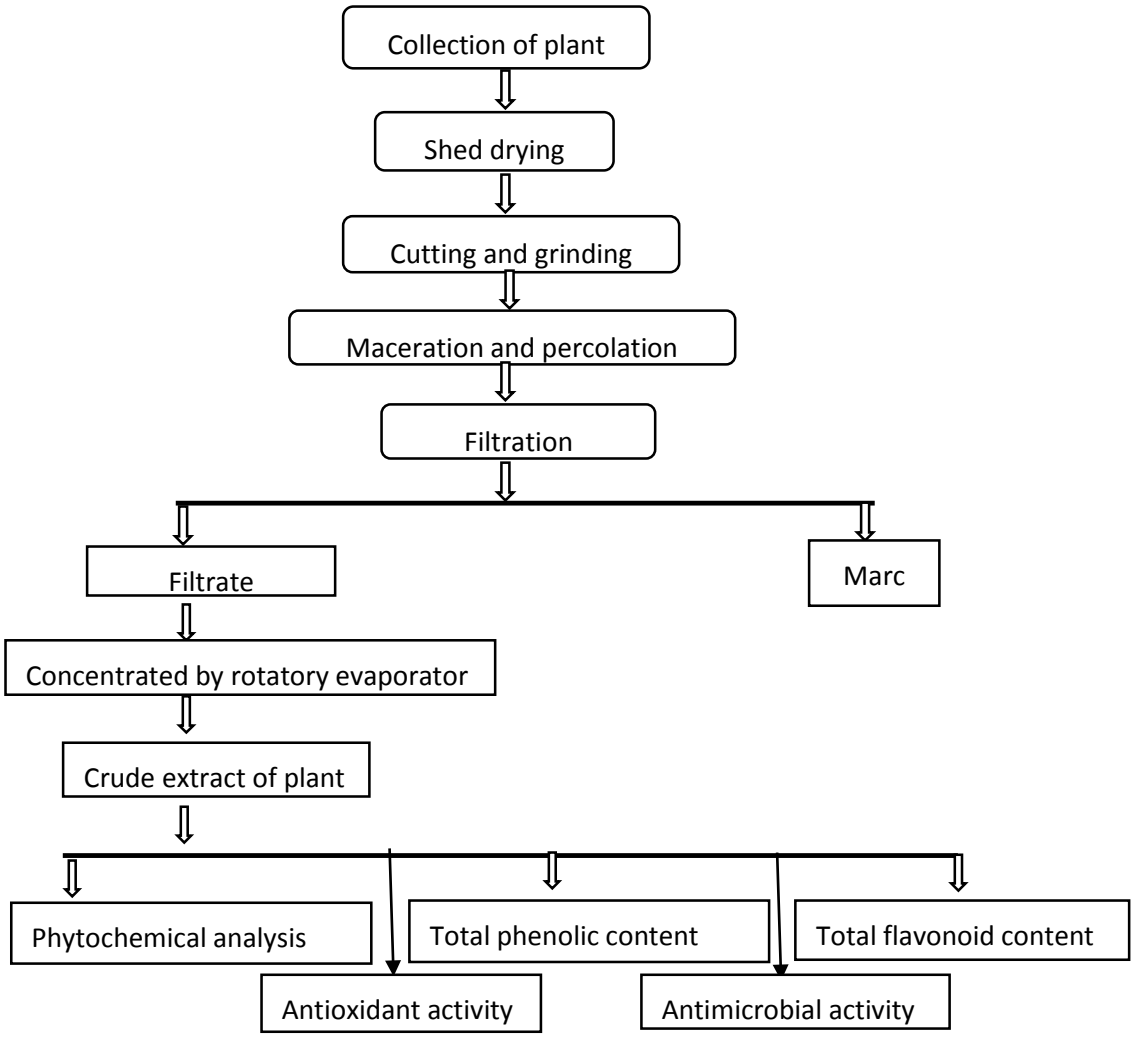

Figure 6: Flow chart showing the methodology of the research

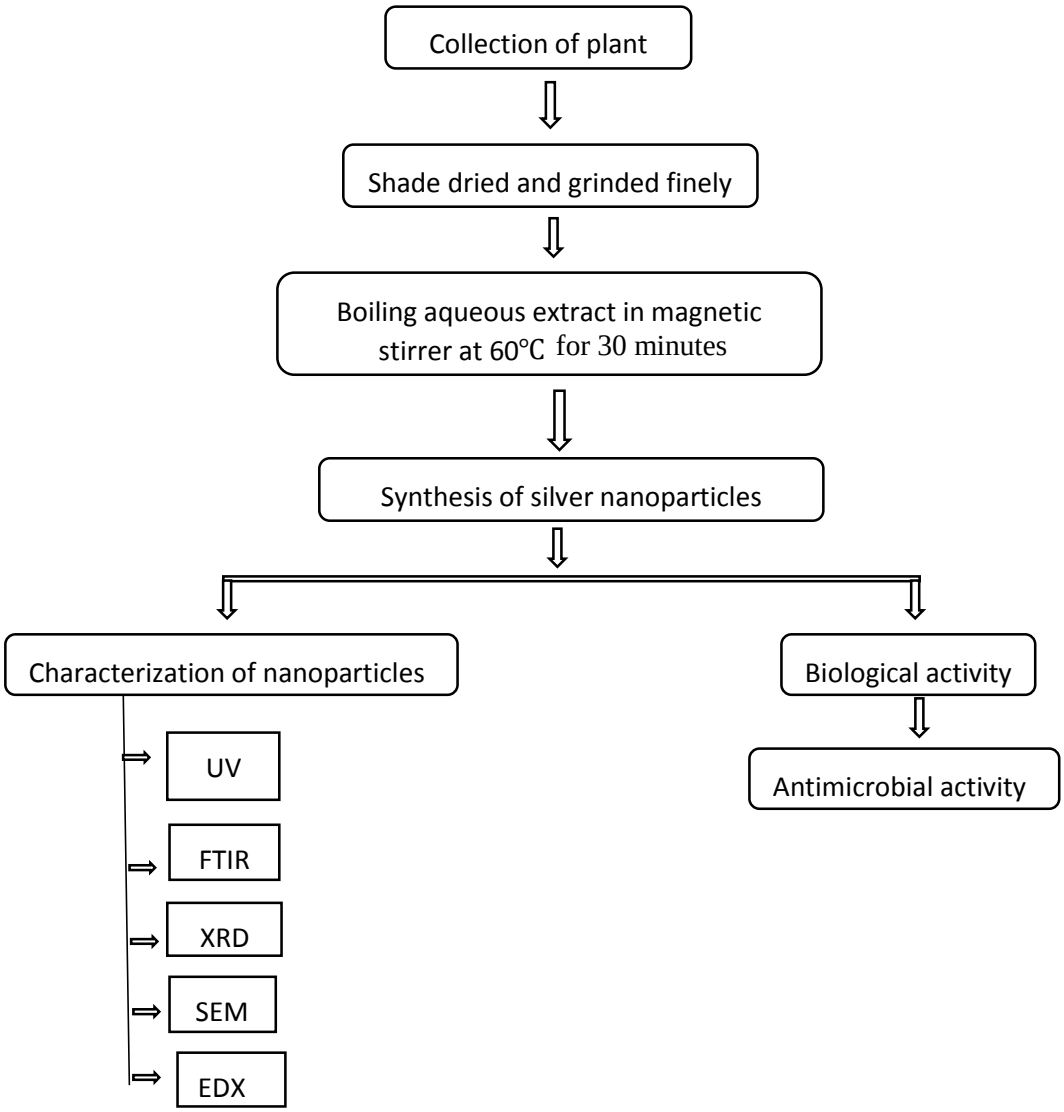

Figure 7: Flow chart showing the synthesis of AgNPs

3.3 Phytochemical analysis

The different phytochemicals present in the plant *Rhus chinensis* were tested using the extract that had been prepared. Required chemical reagents were prepared and specific tests were conducted for particular phytochemicals. The screening process is mostly based on the protocol that is generally followed (Sharma et al., 2020) and (Kalita et al., 2011). The procedure is mentioned in the following Appendix.

3.4 Estimation of total phenolic content (TPC)

The total phenolic content of the plant extract of *Rhus chinensis* was estimated by the Folin-Ciocalteau phenol reagent involving gallic acid as the standard based on

oxidation-reduction reaction. The procedure carried out for the total phenolic content was based on the standard protocol (Kupina et al., 2018)

3.4.1 Preparation of reagent

1M anhydrous sodium carbonate (Na_2CO_3) solution was prepared by dissolving 10.6 g in a 100 mL volumetric flask and marking it up to the level with distilled water. FolinCiocalteau phenol reagent (FCR): 10 mL 10% of FCR (1:10v/v) was prepared. For that 1 mL of FCR reagent was added to 9 mL distilled water.

3.4.2 Preparation of standard gallic acid stock solution

Firstly, a stock solution of gallic acid was prepared by dissolving 1mg gallic acid in 1 mL ethanol to make 1000 ppm. Different concentrations of gallic acid like 10, 20, 30, 40, 50, 60, 70, and 80 µg/mL were prepared by serial dilution. During analysis, freshly prepared gallic acid should be used.

3.4.3 Preparation of sample solution

5 mg of concentrated plant extract was dissolved in 1000 µL of 50% DMSO solution. Firstly, 20 µl of standard gallic with various concentrations of 10, 20, 30, 40, 50, 60, 70, and 80 µg/mL were put in triplicate into 96-well plates. 20 µL of plant sample was loaded in triplicate into 96-well plates. Then, 100 µL of Folin-Ciocalteu phenol reagent was loaded in triplicate into 96-well plates. The FCR was used to quantify the total phenol concentration using 96-well plates. After completion of loading 100 µL FCR initial reading was taken at 765 nm. Following that 80 µL of Na_2CO_3 was added individually to each well holding the standard and sample to get a total volume of 200 µL. using a microplate reader, the final absorbance was measured at 765 nm after being left in the dark for 30 minutes. Standard gallic acid was used for constructing the standard curve. Using a gallic acid standard curve, the total amount of polyphenols in the extracts were computed and expressed as milligram of gallic acid equivalent per gram of dry weight (mg GAE/g) of the extract.

3.4.4 Calculation of total phenolic content (TPC)

By using the following relation, the total phenolic content of the extract was calculated for individual extract and expressed as milligrams of gallic acid equivalent per gram of dry weight (mg GAE/g) of extract.

$$C = cV/m \quad \text{(i)}$$

Where,

C = total phenolic content in (mg/g) in gallic acid equivalent (GAE)

c = concentration of gallic acid established from the calibration curve (mg/mL)

V = volume of extract (mL)

m = weight of the plant extract (g)

3.4.5 Statistical analysis

A linear correlation coefficient (R^2) value was derived from the data, which were recorded as the means of three measurements of absorbance for each concentration. The regression equation was given as;

$$y = mx+c \quad \text{(ii)}$$

Where,

y = Absorbance of extract

m = Slope from the calibration curve

x = Concentration of extract

c = Intercept

It was possible to determine the concentration of extracts using the regression equation. The total phenolic content was thus estimated from the concentration value of each extract by the given equation (ii)

3.5 Estimation of total flavonoid content (TFC)

The TFC of plant extracts was determined by following a standard protocol (Wuttisin & Boonsook, 2019). For aluminum chloride colorimetric method involving quercetin as standard.

3.5.1 Preparation of reagent

1 g of $AlCl_3$ was dissolved in 10 mL of distilled water to make 10% aluminum trichloride, and 1M sodium acetate was prepared by dissolving 0.82 g of sodium acetate into 10 mL of distilled water.

3.5.2 Preparation of standard quercetin

1.54 mg quercetin was prepared by dissolving in 10 mL distilled water to make 154 µg/mL concentration of a stock solution. The final concentration of 10, 20, 30, 40, 50, 60, 70, 80, 90, and 100 µg/mL was prepared by diluting stock solution.

3.5.3 Preparation of sample

5 mg of concentrated plant extract was dissolved in 1000 µL of 50% DMSO solution.

First of all, 130 µl of different quercetin concentrations (10, 20, 30, 40, 50, 60, 70, 80, 90, and 100 µL) were loaded triplicate in 96-well plates. Similarly, 20 µL of plant sample (5000µg/ml) was loaded in triplicate and 110 µL of distilled water was loaded in each well containing plant sample. The initial reading was taken at wavelength 415 nm. Following that, 5 µL $AlCl_3$, 5 µL sodium acetate, and 60 µL ethanol were added separately to each well holding the standard and sample to get a total volume of 200 µL. using a microplate reader, the final wavelength was measured at 415 nm after being left in the dark for 30 minutes. Standard quercetin was used for constructing the standard curve. Using a quercetin standard curve, the total amount of flavonoids in the extracts was computed and expressed as milligrams of quercetin equivalent per gram of dry weight (mg QE/g) of the extract.

3.5.4 Calculation of total flavonoid content (TFC)

By using standard protocols, the total flavonoid content of the extract was calculated for individual extract and expressed as milligrams of quercetin equivalent per gram of dry weight (mg QE/g) of extract.

$$C = cV/m \quad \text{(i)}$$

Where,

C = Total flavonoid content in (mg/g) in quercetin equivalent (QE)

c = concentration of quercetin established from the calibration curve (mg/mL)

V = volume of extract (mL)

m = weight of the plant extract (g)

3.5.5 Statistical analysis

A linear correlation coefficient (R^2) value was derived from the data, which were recorded as the means of three measurements of absorbance for each concentration. The regression equation was given as;

$$y = mx+c \quad \text{(ii)}$$

Where,

y = Absorbance of extract

m = Slope from the calibration curve

x = Concentration of extract

c = Intercept

It was possible to determine the concentration of extracts using the regression equation. The total flavonoid content was thus estimated from the concentration value of each extract by the given equation (ii)

3.6 Determination of antioxidant activity

A quick, easy, and affordable way to evaluate antioxidant activity is to use the free radical 2, 2-Diphenyl-1-picrylhydrazyl (DPPH). Using a common procedure (Chandra et al., 2014), the capacity of several plant extracts to neutralize DPPH free radicals was calculated.

The percentage of radical scavenging activity was calculated by using the following equation.

$$\text{Percentage scavenging (\%)} = [((A_{control} - A_{sample}) / A_{control})] \times 100$$

Where,

$A_{control}$ is the absorbance of the control and A_{sample} is the absorbance of the sample.

3.6.1 Preparation of DPPH solution

1.95 mg DPPH was prepared by dissolving in 50 mL methanol in a volumetric flask to make a 0.1 mM DPPH solution and the prepared solution was covered by aluminum foil.

3.6.2 Preparation of sample

The plant extract was made from a stock solution of 5000 µg/mL solution in 50% DMSO at various concentrations of 100, 50, 25, 12.5, and 6.25 µg/mL. Triplicates of 100 µL of quercetin at various concentrations were loaded as the positive control, and triplicates of 50% DMSO were loaded as the negative control. After loading 100 µl of plant samples at various concentrations, initial absorbance at 517 nm was measured. Following the initial reading, each well received 100 µl of DPPH solution, which was then incubated for 30 minutes in the dark. After incubation, a final reading was taken, and the proportion of the sample that was scavenged was computed. This percentage was then compared to the standard quercetin curve.

$$\text{Percentage scavenging (\%)} = [((A_{control} - A_{sample}) / A_{control})] \times 100$$

Where,

$A_{control}$ is the absorbance of the control and A_{sample} is the absorbance of the sample.

3.7 Antimicrobial activity

Antimicrobial activity was prepared by agar well diffusion method using a standard protocol (Joshi et al., 2020). ZOI (zone of inhibition) was used to define the potential of antimicrobial activity.

3.7.1 Preparation of stock solution

A working solution containing 100 mg/ml of each crude extract was created by thoroughly adding 1 mL of 50% DMSO solvent to a sterile vial holding 100 mg of each extract. The extract was dissolved in 50% DMSO. The stock solution was made, and the tube was sealed and put until needed in a freezer (4℃).

3.7.2 Collection of the test Organism

The detected bacteria strains were from our antimicrobial lab at the Central Department of Chemistry. Gram-positive bacteria *Staphylococcus aureus* ATTC 43300, *Shigella sonnei* ATCC 25931, and Gram-negative bacteria *Klebsiella pneumonia* ATCC 700603 and *Escherichia coli* ATCC 25922 were among the strains used in the study.

3.7.3 Preparation of standard culture inoculums

Using an inoculating loop from the primary culture plate, the test organisms were aseptically handled. After that, it was put into a test tube with 10 mL of sterile liquid nutrient broth and incubated in the incubator for the entire night at 37℃.

3.7.4 Preparation of media

Media was prepared by mixing 38 g of agar in an unsuitable-sized conical flask with distilled water to make a final volume of 1000 mL (38g/liter). After that, it was autoclaved for 15 minutes at 121℃ while being continuously shaken during the boiling process. The sterile material was allowed to cool to around 50℃. They were divided into 25 mL- per-plate, sterile, petri- plated with a diameter of 90 mm, and correctly labeled. The plates were left in their original state to solidify.

3.7.5 Qualitative Screening and Evaluation of antimicrobial activity

A suitable temperature was used to dry prepared sterile Muller- Hilton Agar (MHA) plates to remove extra moisture from the media's surface. The name of the bacteria and the name code of the sample along with the name of the disc were written on the agar plates before they were used in the assay. Using a sterile swab, the bacteria inoculums were placed into petri discs containing solid media of agar. The prepared inoculums were applied to the sterile cotton swab, which was then carefully swiped over the plates to remove any excess by spinning and pressing against the upper interior wall of tubes above the liquid level. After each swab, the plates were turned via a 60° angle. The swab was then used to clean the agar surface's margins. The inoculation plates were kept at room temperature with the lid closed for minutes to allow drying. Using a sterile cork borer, three wells were created in each incubated media plate. The well's diameter was 6 mm, and it was appropriately labeled. With the aid of a micropipette, 50 µL of the plant extract working solution, 50 µL of DMSO as a negative control (N), and 50 µL of the antibiotic neomycin as a positive control (P) were simultaneously poured into each well. The plates were then kept covered for 30 minutes to allow the extract to permeate the media. Overnight, the plates were incubated at 37℃. The presence of bacterial growth inhibition, which is shown by a clear zone surrounding the wells, was checked on the plates after 24 hours of incubation. The zone of inhibition's size was evaluated, and the antibacterial activity was expressed as a function of the zone of inhibition's average diameter, measured in millimeters. It was assumed that there was

no activity if there was no zone of inhibition. Using a millimeter ruler, then the ZOI was measured.

3.7.6 Antimicrobial assay for silver nanoparticles

Disk-diffusion method was used to determine antimicrobial assay for silver nanoparticles. Synthesized powdered form silver nanoparticles of RC-root and leaf were dissolved in concentration at 50 µg/ml in distilled water and left for sonication until it was fully dissolved. 20 µL of silver nanoparticle stock solution was introduced on the Whatmann's filter paper discs of 6mm to make paper discs and then dried for 10 minutes. 1 mg/ml of neomycin and distilled water were used as positive and negative control and prepared separately in different tubes. In this study, Gram-positive bacteria Staphylococcus aureus ATTC 43300 and Gram-negative bacteria *Klebsiella pneumonia* ATCC 700603 were taken as test microorganisms. Using a sterile cotton swab, bacterial culture taken from the suitable inoculums was uniformly distributed over the Petri plates containing Muller- Hilton bacteria to assess the antimicrobial activity of plant extract and synthesize silver nanoparticles of RC-root and leaf extracts. Then, both plant extract and synthesized silver nanoparticles were put on the outer layer of the plates and cultured for a day at the temperature of 37℃. A scale ruler was used to calculate the ZOI.

3.8 Synthesis of silver nanoparticles

Silver nanoparticles were synthesized using a standard protocol (Jalab et al., 2021).

First of all, 5 g of fine powdered form of *Rhus chinensis* parts such as leaves, and roots were well combined with 100 mL deionized water in a conical flask before boiling at 60℃ for 30 minutes while being constantly stirred by a heated magnetic stirrer. The combination was filtered and cooled. For the manufacturing of silver nanoparticles, the resulting aqueous extract was deposited at 4℃. In the first round of analyses, different concentrations of the plant extract were allowed to react with the 1 mM silver nitrate solution in the following ratios: 1:10, 1:9, 1:8, 1: 5, 1:4.and 1:1. After being stirred for 20 minutes using a magnetic stirrer, the solution was stored in the dark. The color change from pale yellow to reddish-brown provided preliminary evidence that silver nanoparticles had formed. In the UV-visible range of 300-700 nm, the UV spectra were recorded at three-time intervals, namely 0 h, 24 h, and 72 h to check the stability of silver nanoparticles. The optimal ratio of plant extract to 1 mM silver nitrate solution

and the best time for nanoparticle production was calculated to be a 1:10 ratio for the leaves part whereas a 1:4 ratio for root and fruit parts with a reaction duration of 24 hours.

In the second round of analysis, a conical flask containing 40 mL, 100 mL of AgNO3 (1 mM) solution, and 10 mL of plant extract (1:4 and 1:10) ratio was added. The mixture was continually stirred for 20 minutes. Based on the color change of the reaction mixture from light yellow to intense reddish brown, which confirms the creation of the silver nanoparticles in the solution, the reaction progression for the synthesis of silver nanoparticles was evaluated. Using a UV-vis spectrophotometer, the mixture was looked at between 300 and 600 nm at various incubation times, and the absorption peak was seen.

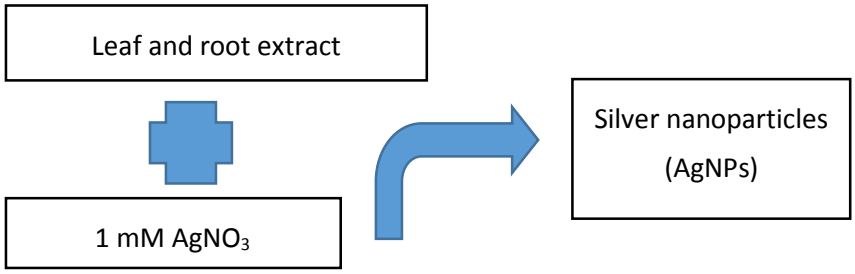

Figure 8: Procedure for synthesizing silver nanoparticles

3.9 Characterization of silver nanoparticles

The characterization evaluation of silver nanoparticles was performed to examine the size, shape, element constituents, color mapping, functional group, crystallinity, and quantity of the particles.

3.9.1 UV-vis spectroscopy

Using a UV-visible spectrophotometer [SPECORD 200 PLUS, (An Endress+Hauser

Company)], the samples' absorption spectra were examined at wavelengths between 300 and 600 nm, and the absorption peak was seen, confirming the creation of silver nanoparticles.

3.9.2 Fourier transfer infrared (FTIR) spectroscopy

Utilizing FTIR analysis, the organic functional group on the surface of the silver nanoparticles, as well as plant extract, was identified, and the spectra were scanned in the range of 400 and 4000 cm^{-1} and all the data obtained were analyzed by using Origin 2019b (9.65) software.

3.9.3 X-ray diffraction analysis

Freeze-dried AgNPs fine powders were employed for XRD analysis utilizing an X-ray diffractometer (D2phaser Bruker, NAST, Nepal) using wavelength 1.540 Å and 30kV voltage to determine and confirm the crystal structure of AgNPs. The working conditions were typically 2θ scanning between 10° to 20°and all the data obtained were analyzed by using Origin 2019b (9.65) software.

Scherer's equation was used to find the size of the crystal as

$$D = \frac{k\lambda}{\beta\cos\theta}$$

Where,

D = crystalline grain size,

k = dimensionless shape factor, with a value close to unity,

λ = wavelength of x-ray radiation

θ = Bragg's angle (half of the 2θ value of chosen peak), and

β = full width at half maximum, FWHM (θ and β should be inradians)

3.9.4 Field emission-scanning electron microscopy (FE-SEM)

The magnified images of the size, shape, composition, crystallography, and other physical and chemical properties of the specimen were determined by using scanning electron microscopy (SU-70 instrument, Korea). The particle size of silver nanoparticles was also determined by using ImageJ software**.**

3.9.5 Energy dispersive X-ray analysis (EDX)

An energy dispersive x-ray analysis technique was used to identify the presence of elemental composition of materials. In addition, EDX analysis, as well as FE-SEM, were used to detect the presence of silver metal.

3.10. Thin layer chromatography (TLC)

TLC is a preliminary test that is frequently used for sample screening before utilizing confirmatory procedures and in an environment with limited resources (Mwankuna et al., 2023). First of all, by using a micropipette, aliquots of 5 µL of two/three spots of each sample extract were spotted on the TLC plates. Then the plates were placed in a glass chamber with developing solvent. Here developing solvent was 15% and 30% ethyl acetate in hexane. Chromatograms were observed on UV light where several multiple spots were seen when which indicated that such extract consists of several phytoconstituents this was just a preliminary assumption. One of the basics of its best solvent extract was taken for further analysis.

CHAPTER -4

RESULTS

The crude extract of different solvents like hexane, DCM, ethyl acetate, methanol, and aqueous solvent was subjected to varying polarity order.

The percentage yield of various extract

$$\% \text{ yield} = \frac{\text{Dry weight of sample powdered}}{\text{A dry weight of crude extract}} \times 100$$

Table 1: Percentage yield of crude extract

Solvent extracts	**Yield% (Leaf)**	**Yield% (Bark)**	**Yield% (Fruit)**	**Yield% (Root)**
Hexane	6.2	12.36	17.38	5.15
DCM	9.58	13.04	15.78	5.32
Ethyl acetate	7.8	12.81	22.18	7.7
Methanol	31.22	6.81	22.44	16
Aqueous	30.23	26.94	21.61	20.1

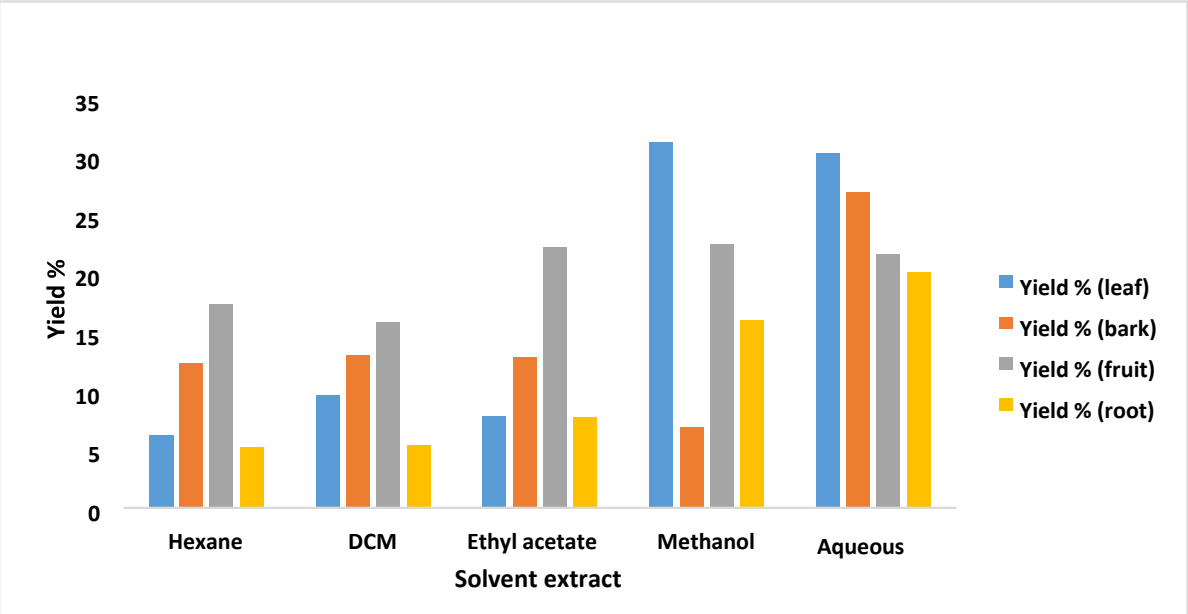

Figure 9: Yield percentage of various extracts

4.1 Qualitative phytochemical analysis

The result of the phytochemical analysis of *Rhus chinensis* leaves, bark, fruit, and root extracts was illustrated by the following table:

Table 2: Qualitative phytochemical analysis of *Rhus chinensis*

SN	Phytochemical test	Crude extract of Leaves	Crude extract of Bark	Crude extract of Fruit	Crude extract of Root
1	Tannins	+	+	+	+
2	Flavonoids	+	+	+	+
3	Saponins	+	+	+	+
4	Carbohydrates	+	+	+	+
5	Glucosides	+	+	+	+
6	Terpenoids	+	+	+	+
7	Alkaloids	+	+	+	+
8	Phenolic	+	+	+	+
9	Quinine	+	+	+	+
10	Volatile oil	+	+	+	_

+ indicates presence, - indicates absence

4.2 Estimation of total phenolic content

For the quantitative determination of total phenols, the Folin- Ciocalteu phenol reagent in terms of the gallic acid equivalent method was used. It involves the oxidation of phenol in an alkaline solution by the yellow reagent made of a solution of sodium molybdate, sodium tungstate, and phosphoric acid, followed by colorimetric detection of the resulting molybdenum tungsten –blue. When the polyphenols in the plant extracts reacted with a particular redox reagent (FCR), they created a blue complex that, depending on the quantitative makeup of the phenol mixture, demonstrated a significant amount of light absorption at 765 nm. The intensity of light absorption at that wavelength is proportional to the concentration of phenols. Here, X-axis is plotted for concentration, and Y- the axis for absorbance. Various final concentrations of gallic acid (10, 20, 30, 40, 50, 60, 70, 80 µg/mL) are used to construct the calibration curve. The regression equation ($Y= 0.0041x$, $R^2 = 0.9863$) derived from the standard gallic

acid calibration curve is used to calculate the TPC of extracts. The TPC value of *Rhus chinensis* was found to be 141.480 ± 0.665 mg GAE/g in a methanolic crude extract of the root part. The numerical data is shown in Annex

The calibration curve for standard gallic acid in terms of absorbance versus concentration is shown in the figure and the TPC value of all extracts is represented in the table below:

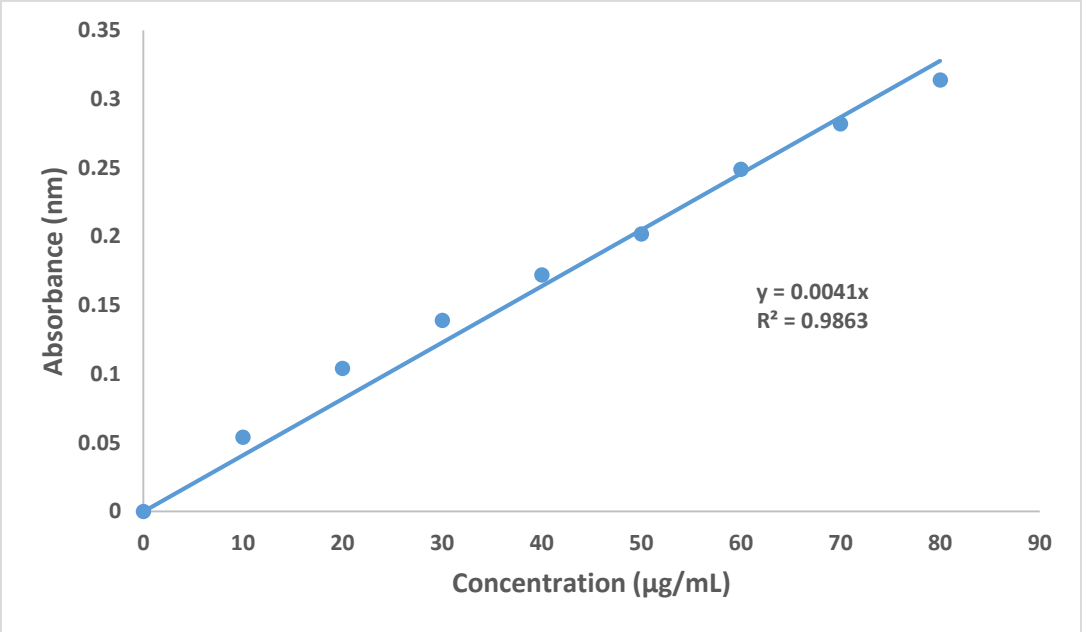

Figure 10: Calibration curve for standard gallic acid.

Table 3: Total phenolic content of different parts of *Rhus chinensis* in different solvents

Crude extracts	**TPC (leaves) (mg GAE/g)**	**TPC (bark) (mg GAE/g)**	**TPC (fruit) (mg GAE/g)**	**TPC (root) (mg GAE/g)**
Hexane	6.179 ± 1.141	2.911 ± 0.889	3.415 ± 0.195	6.667 ± 0.772
DCM	6.927 ± 0.923	12.715 ± 1.310	4.504 ± 0.564	18.163 ± 1.547
Ethyl acetate	15.057 ± 0.676	114.732 ± 0.197	95.577 ± 1.141	131.089 ± 0.282
Methanol	132.000 ± 1.199	137.154 ± 2.513	104.195 ± 0.425	141.480 ± 0.665
Aqueous	33.024 ± 0.762	73.138 ± 1.058	18.488 ± 0.509	138.585 ± 1.942

The obtained TPC values of different parts of *Rhus chinensis* had been expressed in pictorial form as a comparative bar diagram for the easy interpretation of data.

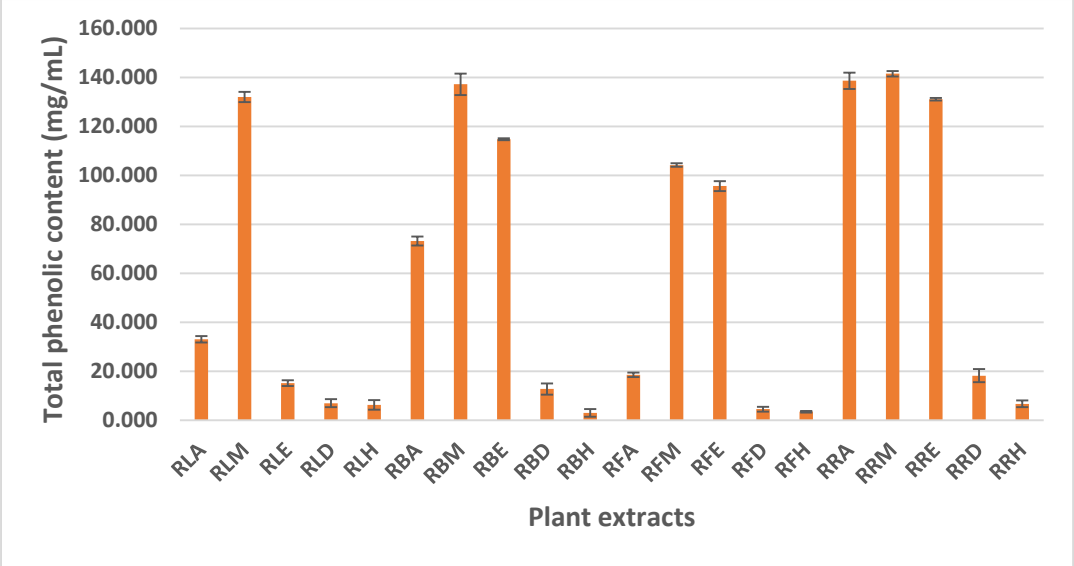

R= *Rhus chinensis*, L= Leaves, B=Bark, F= Fruit, R= Root, A= Aqueous, M= Methanol, E= Ethyl acetate, D= DCM, H=Hexane.

Figure 11: TPC values of different extracts of *Rhus chinensis*

From above table 3 and the comparative analysis of different parts of *Rhus chinensis* it was clear that this plant is rich in phenolic content which corresponds to various literature and TPC value ranged from the lowest value of 2.911 ± 0.889 mg GAE/g which was found in hexane crude extract of bark part to the highest value of 141.480 ± 0.665 mg GAE/g in methanol extract of root part.

Phenolic compounds exhibit excellent antioxidant capabilities as a result of their capacity to scavenge free radicles. It has been claimed that higher polyphenol concentration directly correlates with higher antioxidant activity. However, when phenolic compounds are quantified in plant extracts, their structural characteristics, variation in plant samples, various analytical assay methods, choice of standard, and methodology followed may result in distinct or altered TPC values.

4.3 Total flavonoid content (TFC)

For the quantitative determination, the aluminum chloride colorimetric assay was used for the estimation of the total flavonoid content of various crude extracts of *Rhus chinensis* by using a standard protocol, which includes quercetin as a standard. Quercetin equivalent (mg QE/g of the dry weight of extract) is used to express TFC value. The plant extract's flavonoids form compounds with bright yellow fluorescence when aluminum chloride is present, as may be seen using a UV spectrophotometer at

415 nm. The calibration crude was prepared by using various final quercetin concentrations (100, 90, 80, 70, 60, 50, 40, 30, 20, and 10). The regression equation (Y= 0.0029, R^2 = 0.9859) derived from the quercetin calibration curve is used to calculate the TFC of extracts. The TFC value of *Rhus chinensis* was found to be 54.345 ± 0.279 mg QE/g in ethyl acetate crude extract of the root part. Here, X-axis is plotted for concentration, and Y- the axis for absorbance. The numerical data is shown in Annex

The calibration curve for standard quercetin in terms of absorbance versus concentration is shown below:

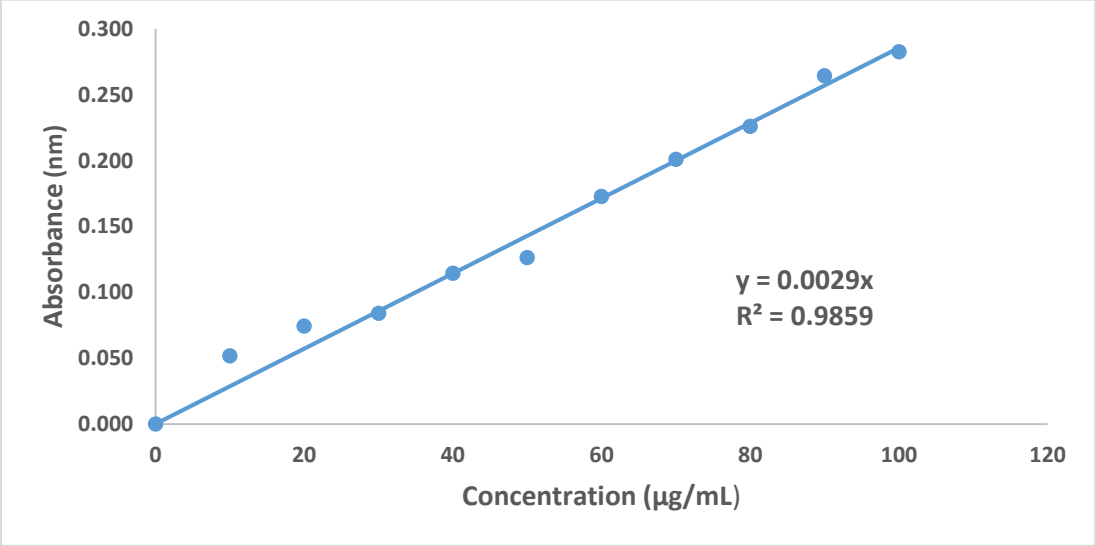

Figure 12: Calibration curve for standard quercetin.

Table 4: Total flavonoid content of different parts of *Rhus chinensis* extracts in different solvents

Crude extracts	**TFC (leaves) (mg QE/g)**	**TFC (bark) (mg QE/g)**	**TFC (fruit) (mg QE/g)**	**TFC (root) (mg QE/g)**
Hexane	8.989 ± 1.680	10.414 ± 1.074	13.862 ± 1.100	44.805 ± 0.140
DCM	19.816 ± 0.587	41.103 ± 0.744	16.437 ± 1.627	28.345 ± 0.222
Ethyl acetate	34.069 ± 1.817	47.310 ± 0.174	26.253 ± 1.807	54.345± 0.279
Methanol	39.609 ± 0.304	8.437 ± 0.876	44.690 ± 0.958	4.552 ± 0.182
Aqueous	8.759 ± 0.211	5.103 ± 0.207	2.345 ± 0.518	29.126 ± 0.809

The obtained TFC values of different parts of *Rhus chinensis* had been expressed in pictorial form as a comparative bar diagram for the easy interpretation of data.

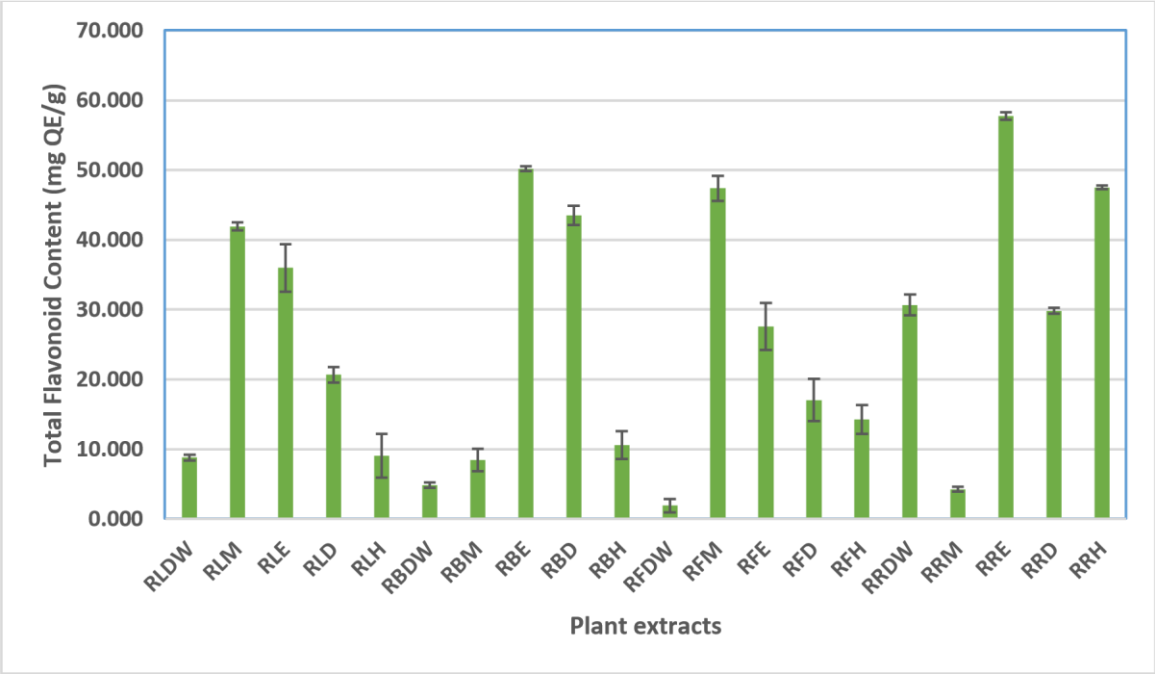

R= *Rhus chinensis*, L= Leaves, B=Bark, F= Fruit, R= Root, A= Aqueous, M= Methanol, E= Ethyl acetate, D= DCM, H=Hexane.

Figure 13: TFC values of different extracts of *Rhus chinensis*

From the above table 4 and comparative analysis of different parts of *Rhus chinensis*, it was clear that this plant is rich in flavonoid content which corresponds to various literature and TFC value ranged from the lowest value of 2.345 ± 0.518 mg QE/g which was found in an aqueous crude extract of fruit part to the highest value of 54.345 ± 0.279 mg OE/g in ethyl acetate extract of root part.

4.4 DPPH radical scavenging activity

The method of scavenging stable DPPH radical is a commonly used method for determining the free radicle scavenging ability of the test component. DPPH radical has a maximum absorption wavelength of 517 nm and is a stable nitrogen-centered radicle. An antioxidant can quickly remove the DPPH by donating hydrogen or electrons. When the DPPH is reduced it turns from violet to yellow. The degree of decolorization indicates the free radical scavenging potentials that are antioxidant potentials of the sample. The free radical inhibition activity of plant extracts at various

concentrations was calculated and a graph of inhibition percentage versus concentration was plotted.

The plant extract's ability to scavenge DPPH is measured by its IC_{50} value which is the concentration needed to inhibit 50% inhibition. The outcomes were compared with quercetin. The standard curve, represented by the nonlinear graph, is based on the inhibition of the DPPH radical by the final concentration of standard quercetin (10, 5, 2.5, 1.25, 0.625, 0.312 g/mL).

The graphical presentation of the inhibition by various extracts and standard quercetin has been shown below in the figure:

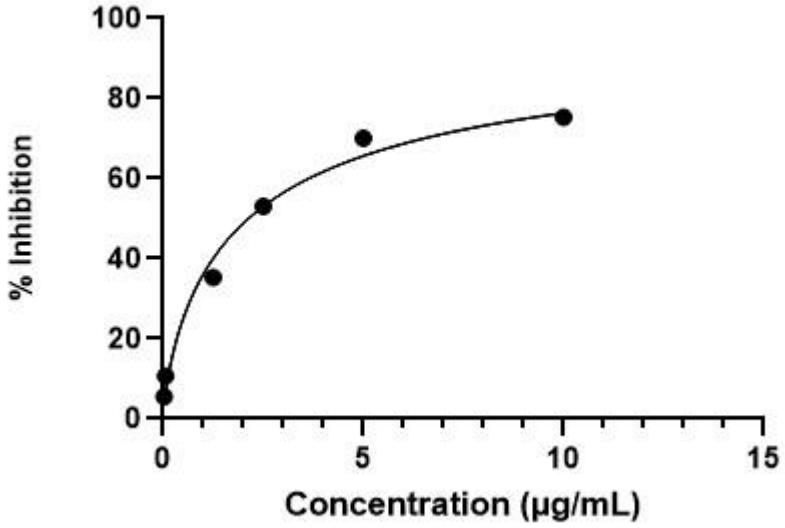

Figure 14: Standard curve of DPPH inhibition by Quercetin

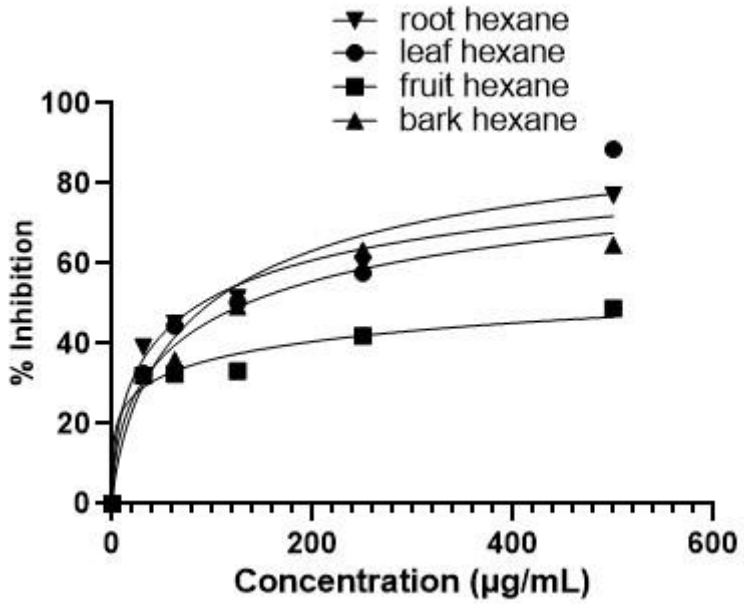

Figure 15: A plot of DPPH inhibition against concentration for hexane crude extract of all parts of *Rhus chinensis*.

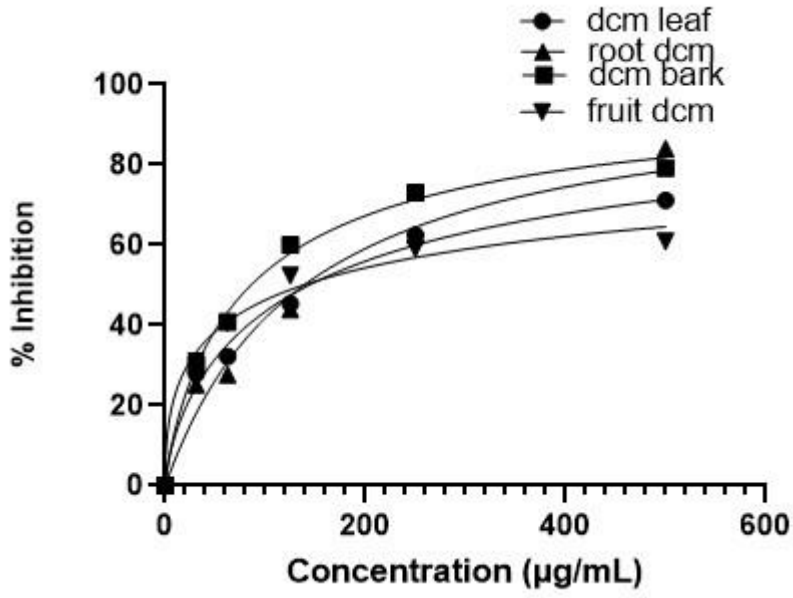

Figure 16: A plot of DPPH inhibition against concentration for DCM crude extract of all parts of *Rhus chinensis*.

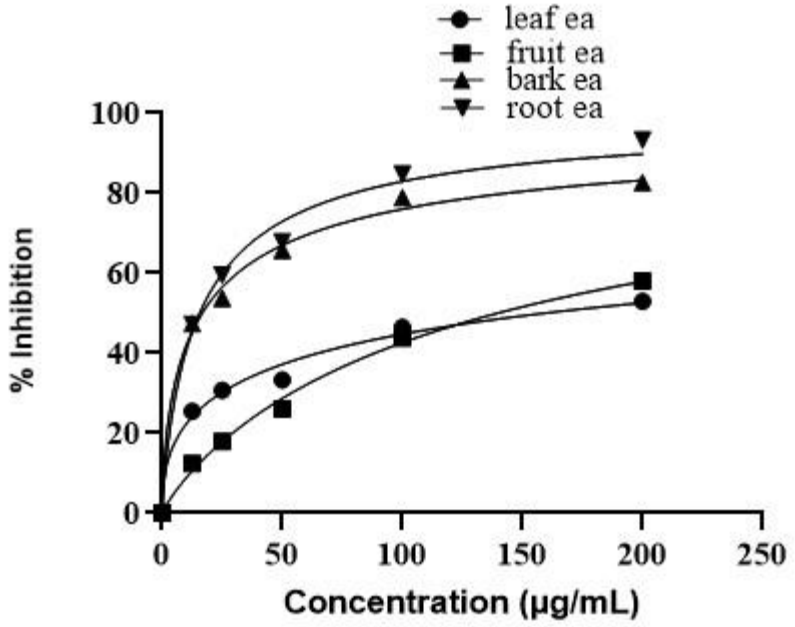

Figure 17: A plot of DPPH inhibition against concentration for ethyl acetate crude extract of all parts of *Rhus chinensis*.

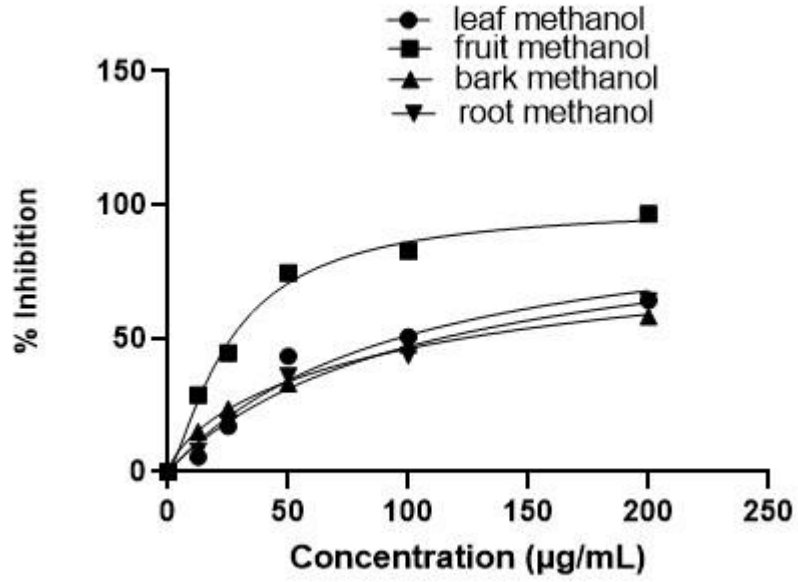

Figure 18: A plot of DPPH inhibition against concentration for a methanolic crude extract of all parts of *Rhus chinensis*.

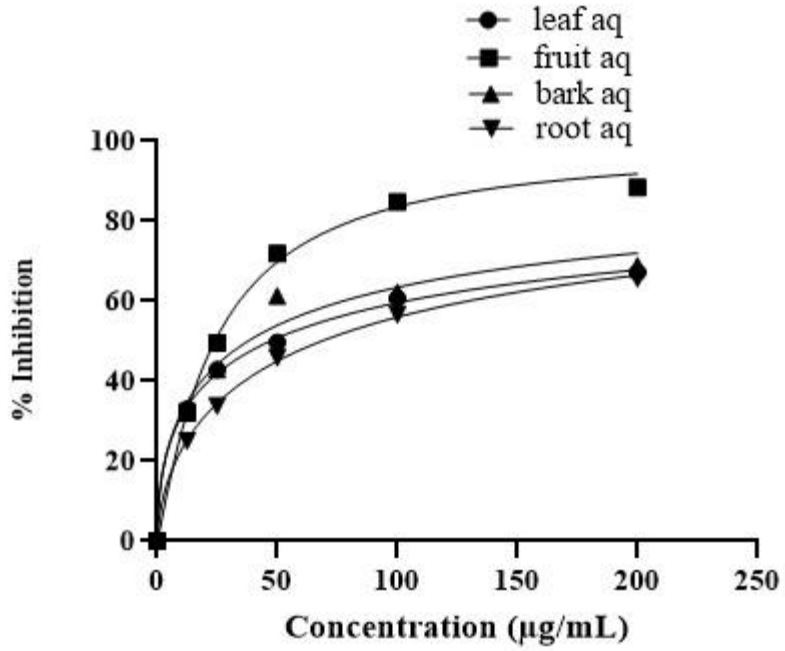

Figure 19: A plot of DPPH inhibition against concentration for an aqueous crude extract of all parts of *Rhus chinensis*.

The amount of each plant extract needed to inhibit DPPH activity by 50% (IC_{50}) was calculated using a linear regression of the percentage of radical scavenging against concentration. The relationship between the antioxidant potential and IC_{50} value is inverse; a lower IC_{50} value denotes a higher antioxidant potential. The IC_{50} value of the plant extract along with the standard quercetin is tabulated below:

Table 5: IC_{50} values of hexane crude extract of different parts of *Rhus chinensis* with standard quercetin

S.N	**Plant extracts**	**IC_{50} (µg/mL)**
1	Quercetin	2.2567 ± 0.296
	RLH	48.763 ± 0.765
	RFH	408.150 ± 0.294
	RBH	66.817 ± 2.605
	RRH	43.903 ± 2.762

Table 6: IC_{50} values of DCM crude extract of different parts of *Rhus chinensis* with standard quercetin

S.N	Plant extracts	IC_{50} (µg/mL)
2	Quercetin	2.2567 ± 0.296
	RLD	72.067 ± 1.069
	RFD	69.068 ± 0.288
	RBD	42.953 ± 0.374
	RRD	69.500 ± 0.693

Table 7: IC_{50} values of ethyl acetate crude extract of different parts of *Rhus chinensis* with standard quercetin

S.N	Plant extracts	IC_{50} (µg/mL)
3	Quercetin	2.2567 ± 0.296
	RLE	79.750 ± 1.835
	RFE	69.933 ± 1.108
	RBE	8.348 ± 0.372
	RRE	7.830 ± 0.187

Table 8: IC_{50} values of methanolic crude extract of different parts of *Rhus chinensis* with standard quercetin

S.N	Plant extracts	IC_{50} (µg/mL)
4	Quercetin	2.2567 ± 0.296
	RLM	47.877 ± 1.657
	RFM	13.143 ± 0.406
	RBM	61.400 ± 0.843
	RRM	56.817 ± 0.960

Table 9: IC_{50} values of aqueous crude extract of different parts of *Rhus chinensis* with standard quercetin

S.N	Plant extracts	IC_{50} (µg/mL)
5	Quercetin	2.2567 ± 0.296
	RLA	23.645 ± 0.580
	RFA	10.117 ± 0.471
	RBA	19.040 ± 1.364
	RRA	34.233 ± 0.331

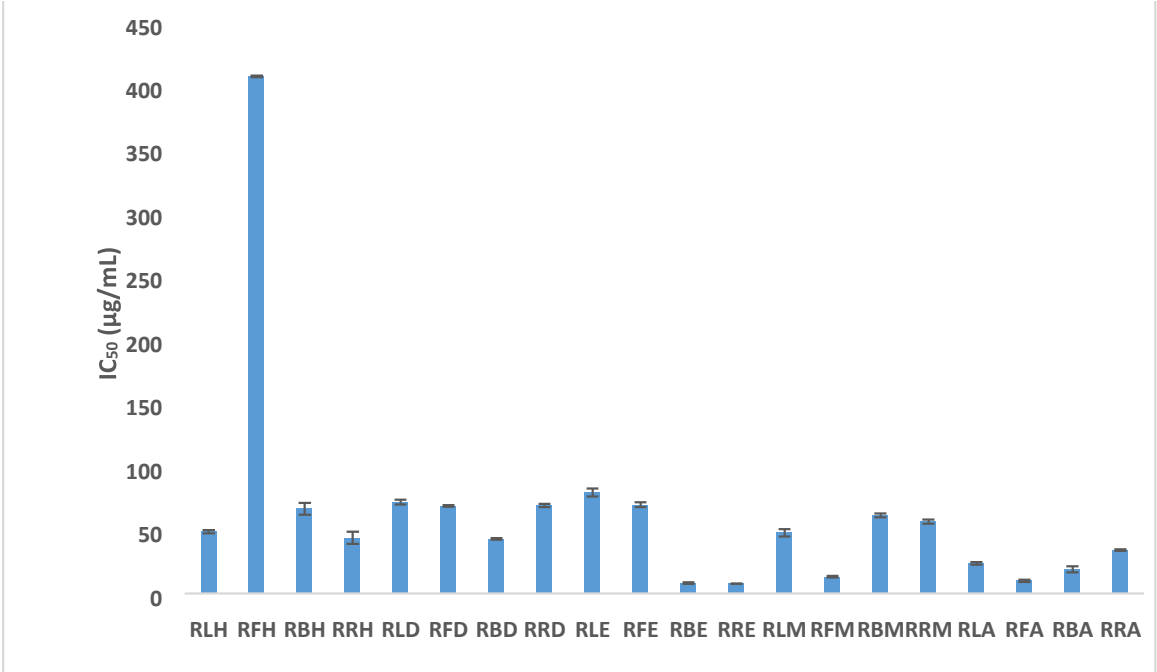

Figure 20: Free radical scavenging activity in different concentrations of plant crude extracts.

The table and the bar diagram showed that the plant extracts were potential antioxidants as their IC_{50} values were found to be close to the standard quercetin of IC_{50} value (2.2567 ± 0.296 µg/mL). Among all, the ethyl acetate crude extract of *Rhus chinensis* root part showed the strongest DPPH scavenging activity as compared to other extracts, as their IC_{50} values were close to standard quercetin. Similarly, the least potent antioxidant was found in hexane crude extract of fruit part of IC_{50} value (408.150 ± 0.294 µg/mL)

The body can develop free radicles, which can harm cells and lead to several diseases, antioxidants from natural sources, like plants can repair and neutralize these free radicles making them incredibly helpful in preventing a variety of diseases. The body can develop free radicals, which can harm cells and lead to several diseases. The findings show that the plant explained above can function as a very good choice in the field of medicine based on the chemistry of antioxidants in natural products.

4.5 Antimicrobial activity

Based on TLC in such a study ethyl solvent extract was used as the best solvent extract than other solvent extracts for the antimicrobial activity because while screening the TLC plate of ethyl acetate extracts of all samples showed many spots when enclosed in a glass vessel in 30% ethyl acetate which might be assumed that it has many secondary metabolites. TLC is a preliminary test that is frequently used for sample screening before utilizing confirmatory procedures and in an environment with limited resources (Mwankuna et al., 2023).

Antimicrobial activity was prepared by agar well diffusion method using a standard protocol. ZOI (zone of inhibition) was used to define the potential of antimicrobial activity. To estimate the antimicrobial activity of plant extracts, the diameter of the zone of inhibition produced on a particular bacterium was evaluated.

Table 10. Antimicrobial screening results of three plant extracts.

Plant extracts	**Names of bacteria**	**Diameter of ZOI of the sample(mm)**	**ZOI of the positive control Neomycin(mm)**
RLE	*Shigella sonnei* ATCC 25931	15	25
	Staphylococcus aureus ATCC 43300	15	25
	Klebsiella pneumonia ATCC 700603	19	30
	Escherichia coli ATCC 25922	25	20
	Shigella sonnei ATCC 25931	15	25
RBE	*Staphylococcus aureus* ATCC 43300	16	25
	Klebsiella pneumonia ATCC 700603	15	30
	Escherichia coli ATCC 25922	14	20

RFE	*Shigella sonnei* ATCC 25931	12	25
	Staphylococcus aureus ATCC 43300	10	25
	Klebsiella pneumonia ATCC 700603	12	30
	Escherichia coli ATCC 25922	12	20
RRE	*Shigella sonnei* ATCC 25931	20	25
	Staphylococcus aureus ATCC 43300	22	25
	Klebsiella pneumonia ATCC 700603	18	30
	Escherichia coli ATCC 25922	-	20

Where ZOI = Zone of inhibition, (-) = no effective antimicrobial activity.

Shigella sonnei ATCC 25931, *Staphylococcus aureus* ATCC 43300 = Gram-positive bacteria

Klebsiella pneumonia ATCC 700603, *Escherichia coli* ATCC 25922 = Gram-positive bacteria

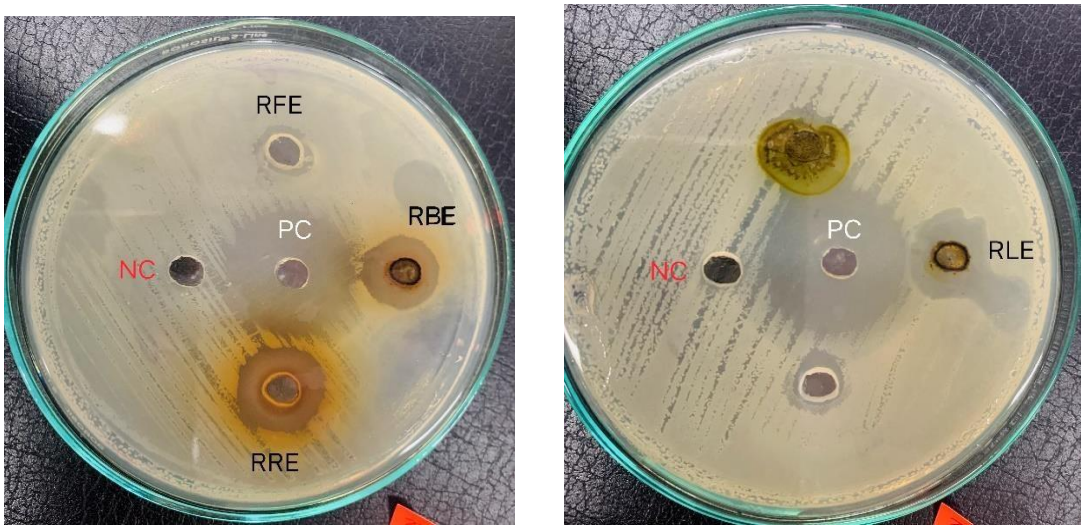

Figure 21: ZOI of the extract against bacteria *Klebsiella pneumonia*

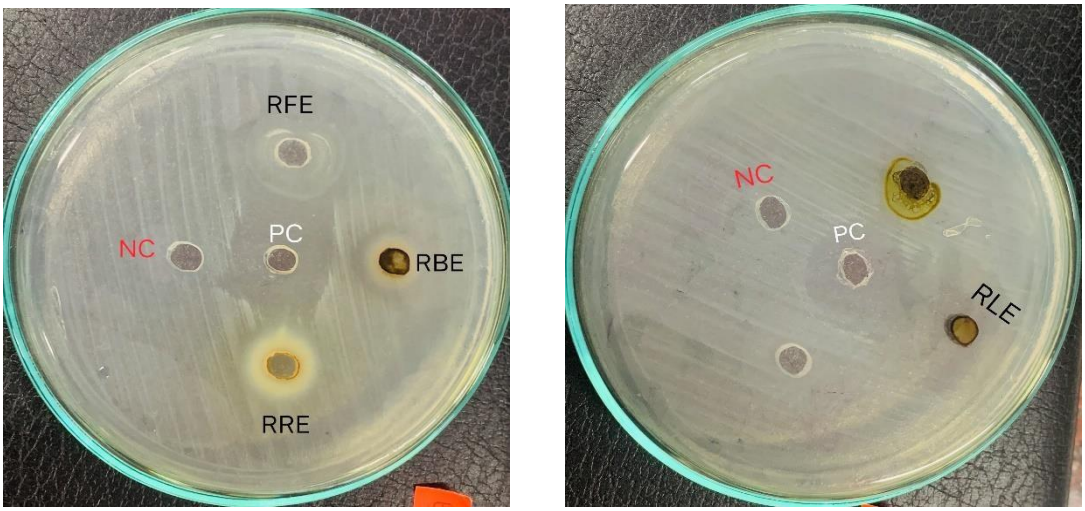

Figure 22: ZOI of the extract against bacteria *Escherichia coli*

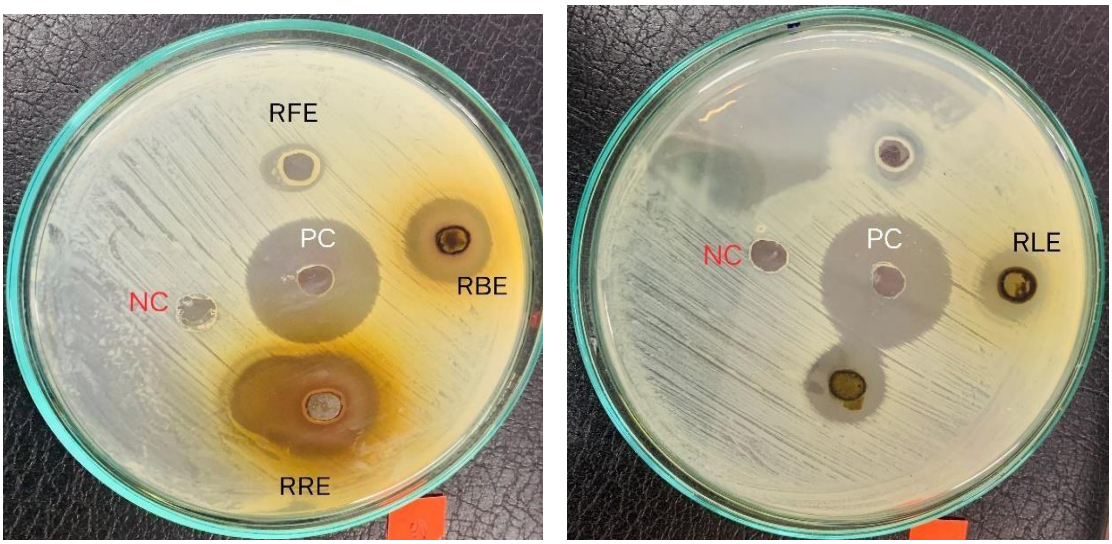

Figure 23: ZOI of the extract against bacteria *Shigella sonnei*

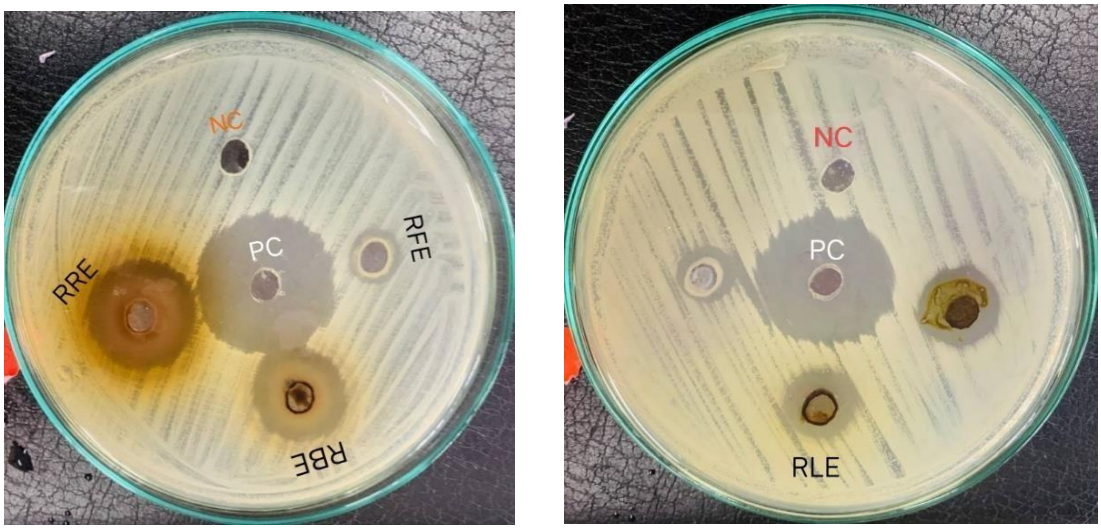

Figure 24: ZOI of the extract against bacteria *Staphylococcus aureus*

The above table indicates that *Rhus Chinese* root was found active against microorganism ATCC 43300 *Staphylococcus aureus* of ZOI 22 mm whereas, ZOI of positive control Neomycin was found to be 25mm. *Rhus Chinese* leaf extract was found effective against ATCC 25922 *Escherichia coli of* ZOI 25 mm respectively and ZOI of positive control Neomycin for these bacteria was found to be 20 mm which is greater than the positive control. Here neomycin was used as positive control and 50% DMSO was used as negative control. Gram-positive bacteria were inhibited more successfully than gram-negative bacteria. This finding can be explained by the fact that Gram-negative bacteria have an exclusive outer membrane that prevents the extract from entering the cell, but Gram-positive bacteria do not.

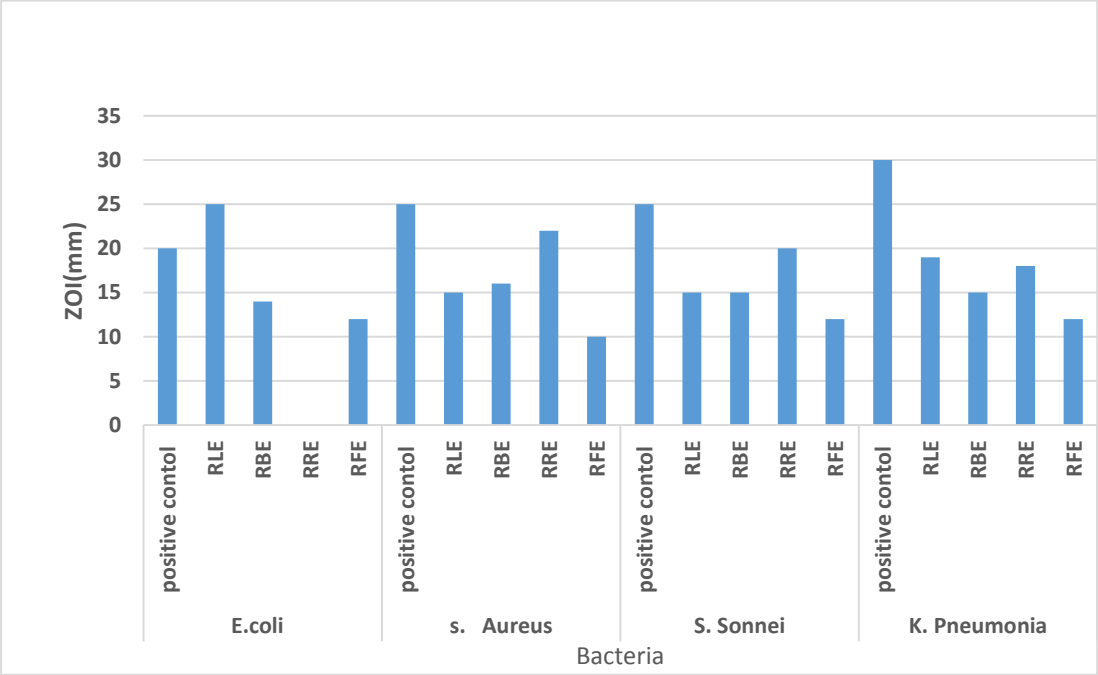

Figure 25: Comparative study of Zone of inhibition (mm) of plant extracts against bacteria

4.6. Green synthesis of silver nanoparticles from RC extract

Silver nanoparticles were synthesized from the aqueous extract of *Rhus chinensis* root and leave parts. The formation of silver nanoparticles was preliminary confirmed by the change of color from light yellow to brown this occurs due to surface Plasmon resonance (SPR). After it, the formed silver nanoparticles were kept in a dark place for 24 hours. After 24 hours then the formed AgNP particles were monitored by UV-visible absorption spectrum under than range of 200 to 600nm.

Figure 26: Visible observation of color change of plant extract after the addition of silver nitrate

4.7 Characterization of silver nanoparticles

4.7.1 UV-Visible spectroscopy

Spectral analysis was performed on the samples after visual confirmation was obtained by seeing a color shift during the biosynthesis of RC-AgNPs. The aqueous extracts of the RC- root and RC- leaf with the silver nitrate solution were observed by UV-visible absorption spectra in the range of 300 to 600 nm to confirm the formation of AgNPs. The Ag^{+} bio-reduced by using UV- visible spectra, the ions in the aqueous extract were observed. The biosynthesized AgNPs of the RC-root sample showed the maximum absorption peak at wavelength 443 nm whereas biosynthesized AgNPs of RC- leaf showed the maximum absorption peak at wavelength 441 nm. Nanoparticles typically exhibit surface Plasmon resonance as a result of the excitation of the free electrons. At 0 hours and 24 hours, it was found to be the most effective period for the creation of stable silver nanoparticles. A UV-visible spectral analysis of the biosynthesized silver nanoparticles of *Rhus chinensis* root and leaf is shown below

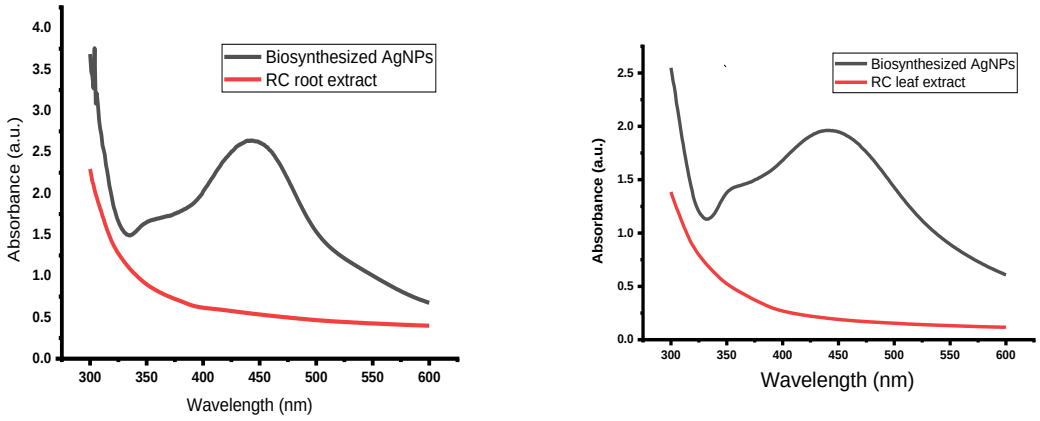

Figure 27: UV-visible spectral analysis of the biosynthesized silver nanoparticles of RC-root and RC- leaf extract.

4.7.2 Fourier transfer infrared spectroscopy (FTIR)

Comparative FTIR spectra were taken between plant extracts and plant extract-capped AgNPs, respectively, and show a shift in peaks for the identification of functional groups, bonding information of biomolecules specifically bonded on the synthesis of AgNPs, and the fraction of hydrogen bonding. FTIR measurements of both the aqueous dried root and leaf extract and their synthesized dried nanoparticles were carried out to identify the possible biomolecules responsible for the reduction of the Ag+ ions and capping of the bio-reduced silver nanoparticles synthesized by root and leaf extract.

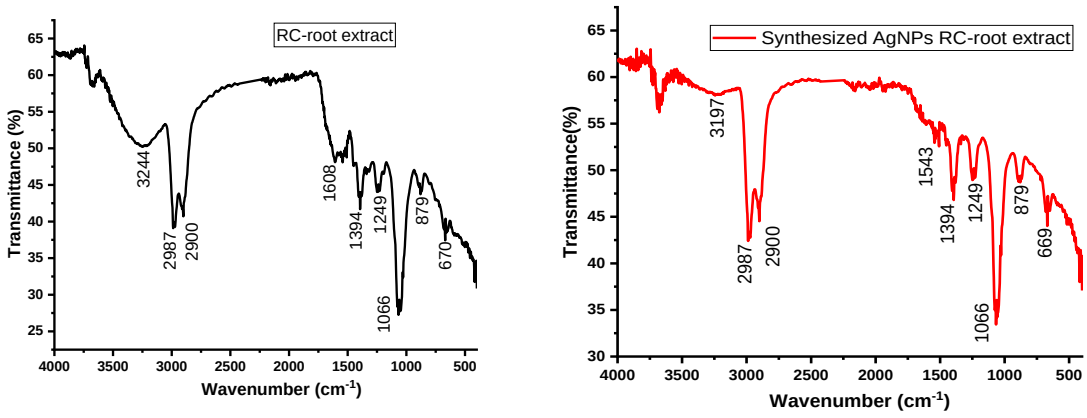

Figure 28: FTIR spectrum of RC-root extract and synthesized AgNPs with RC-root extract.

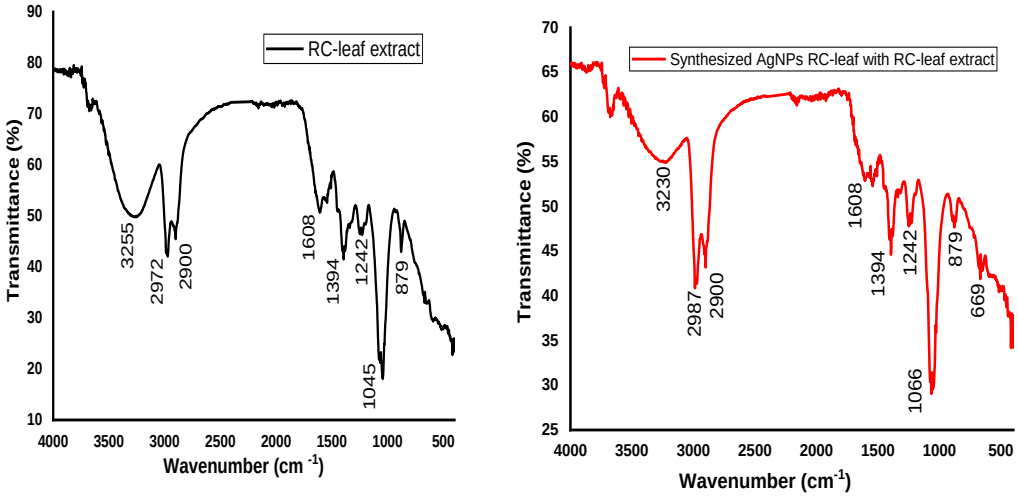

Figure 29: FTIR spectrum of RC-leaf extract and synthesized AgNPs with RC-leaf extract.

The silver nanoparticles using root extract is having -OH stretching and -OH bending assigned at 3197 cm^{-1}, and 1394 cm^{-1}, aromatic C-H stretching and bending group assigned at 2987 cm^{-1}, and 879 cm^{-1}, -C=C stretching occurred at 1543 cm^{-1}, -C-O bonding at 1249 cm^{-1} and C-N bonding occurred at 1066 cm^{-1} respectively. Similarly, as compared to the RC-root extract it showed almost the same peak but a slight change in the –OH bond and it gave a more intense peak as compared to silver nanoparticles. The RC- root extract is having the -OH stretching and -OH bending assigned at 3244 cm^{-1}, and 1394 cm^{-1}, aromatic C-H stretching and bending group assigned at 2987 cm^{1}, and 879 cm^{-1}, -C=C stretching occurred at 1608 cm^{-1}, -C-O bonding at 1249 cm^{-1} and C-N bonding occurred at 1066 cm^{-1} respectively. The silver nanoparticles using leaf extract is having the -OH stretching and -OH bending assigned at 3230 cm^{-1}, and 1394 cm^{-1}, C-H stretching and bending alkane group assigned at 2987 $cm^{-1,}$ and 879 cm^{-1}, -C=C stretching occurred at 1608 cm^{-1}, and, -C-O bonding at 1242 cm^{-1} and C-N bonding occurred at 1066 cm^{-1} respectively. Similarly, as compared to the aqueous RC leaf extract it showed almost the same peak but a slight change in the –OH bond and it gave a more intense peak as compared to silver nanoparticles. The aqueous RC-leaf extract is having the -OH stretching and -OH bending assigned at 3255 cm^{-1}, and 1394 cm^{-1}, C-H stretching and bending alkane group assigned at 2972 cm^{-1}, and 879cm^{-1}, C=C stretching occurred at 1608 cm^{-1}, and, -C-O bonding at 1242 cm^{-1} and C-N bonding occurred at 1045 cm^{-1} respectively.

4.7.3 X-ray diffraction (XRD)

The X-ray diffraction study was used to carry out to establish the crystalline nature of the particles. The XRD spectrum of synthesized AgNPs of RC-root and RC-leaf is shown below in figure no. The XRD pattern of synthesized AgNPs of RC-root has shown four intense peaks corresponding to (111), (200), (220), and (311); Bragg's reflection (2θ = 38.16°, 44.28°, 64.51°, and 77.41. Similarly, AgNPs of RC-root has shown four intense peaks corresponding to (111), (200), (220), and (311); Bragg's reflection (2θ = 38.20°, 44.28°, 64.5°, and 77.44° structure of AgNPs. The average crystallite size of the synthesized RC- root and leaf extract AgNPs was determined using the Debye-Scherer formula to determine the width of each diffraction peak after the Gaussian fitting of all four peaks and was found to be 11.01 nm and 13.39 nm respectively.

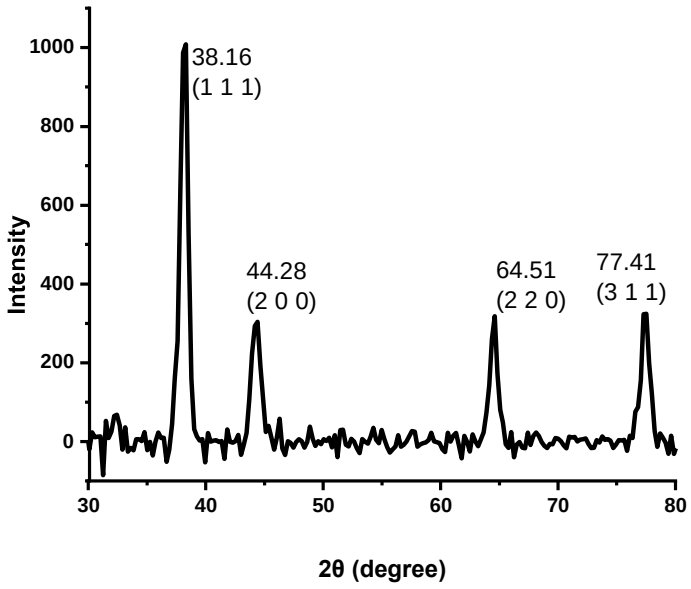

Figure 30: XRD Pattern of synthesized AgNPs by RC-root extract

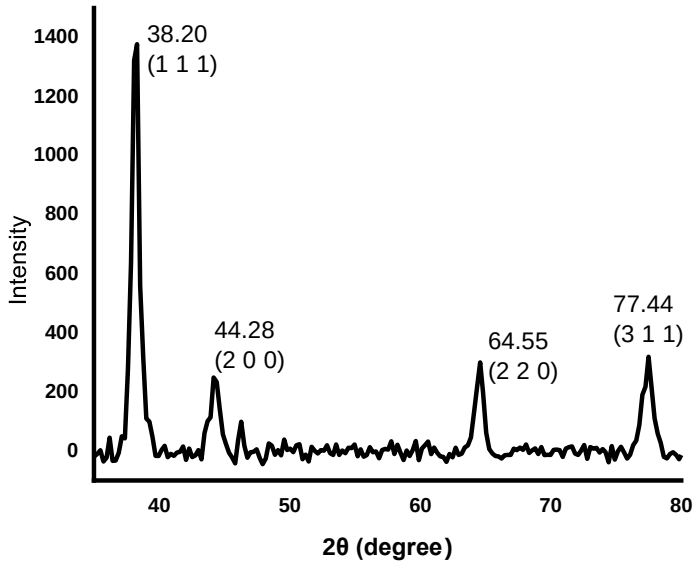

Figure 31: XRD Pattern of synthesized AgNPs by RC-leaf extract

4.7.5 Field emission scanning electron microscopy (FE-SEM)

The FE-SEM was used to analyze the morphological structure as well as to calculate the particle size of nanoparticles. High-density AgNPs were produced by *Rhus chinensis* root and leaf extract, according to FE-SEM examination. It was demonstrated that root extract and leaf extract produced AgNPs with diameters of 54.40 nm and 30.89 nm, respectively. The bioorganic capping molecules that were coupled to the silver nanoparticles interacted with one another via hydrogen bonds and electrostatic interactions to produce the silver nanoparticles' SEM image. The results of the EDX study and the color map were given in the figure below, which proved the presence of the silver component. Through EDX the peak of silver in both AgNPs root and leaf extract showed around 3kev and other elements like Cl, O, C, and N were also reported with synthesized AgNPs.

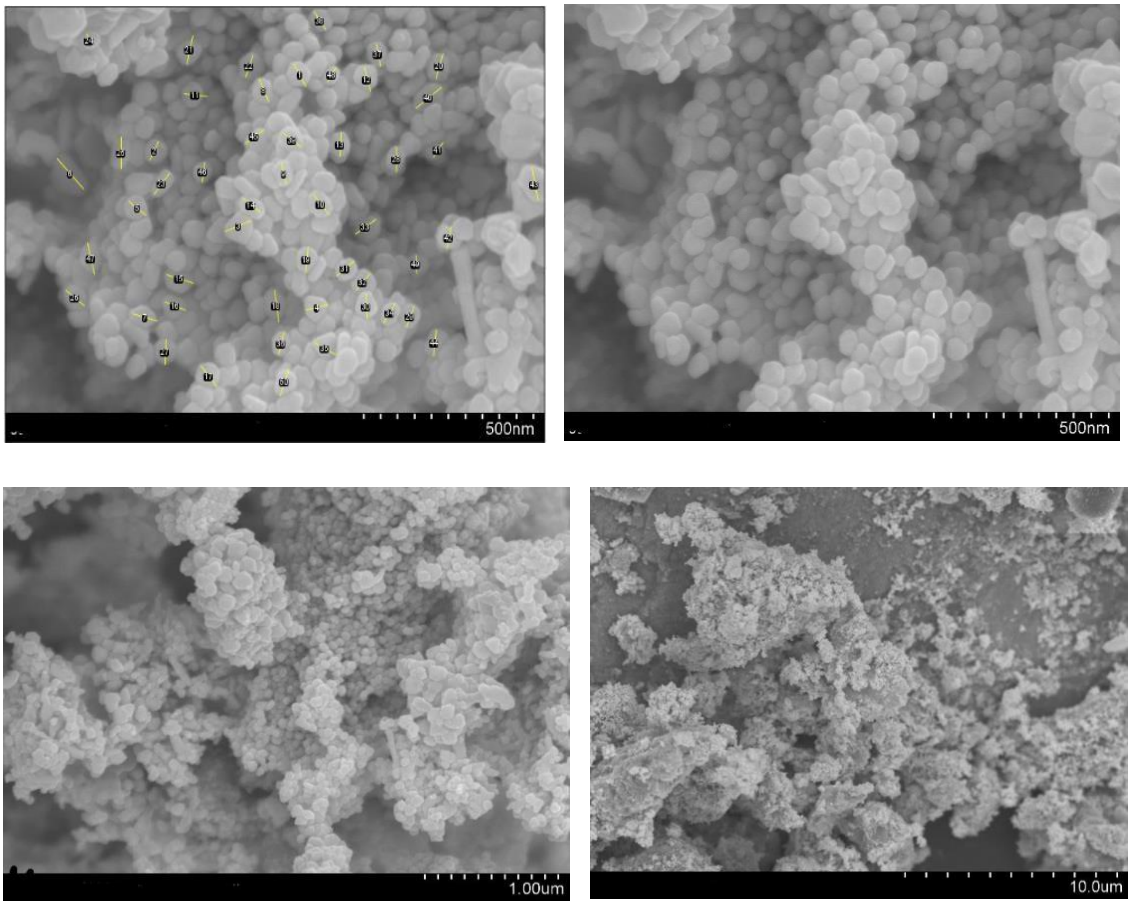

Figure 32: FE-SEM images of synthesized AgNPs using RC root extract.

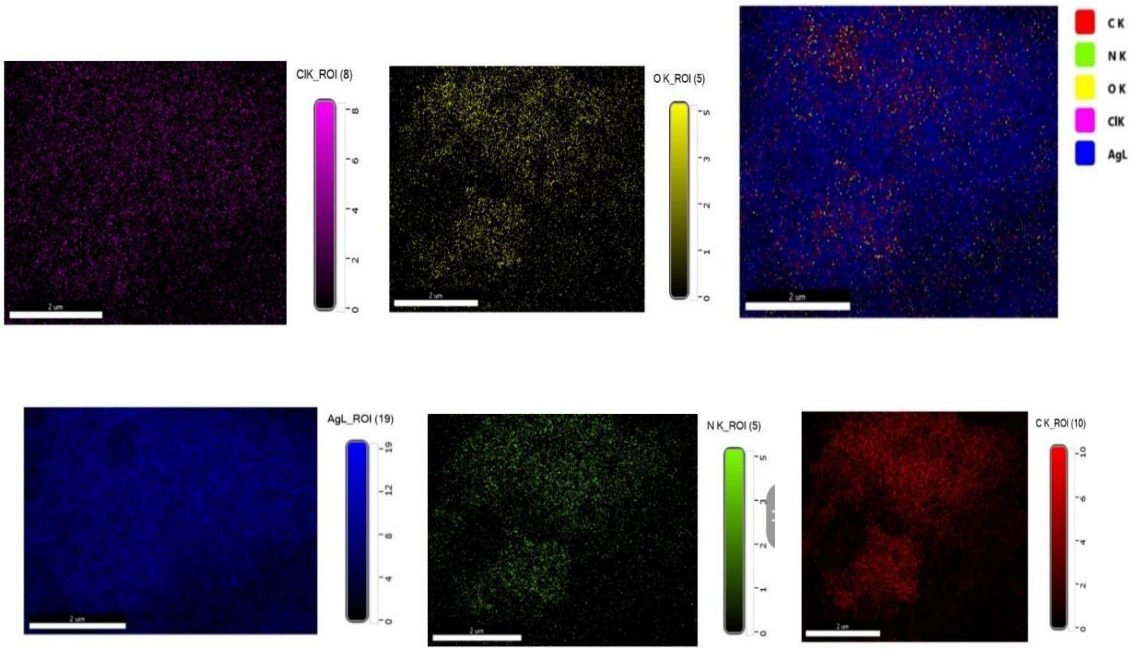

Figure 33: An energy-dispersive x-ray (EDX) spectrum of AgNPs with total elemental mapping and individual color mapping of synthesized AgNPs RC- root extract.

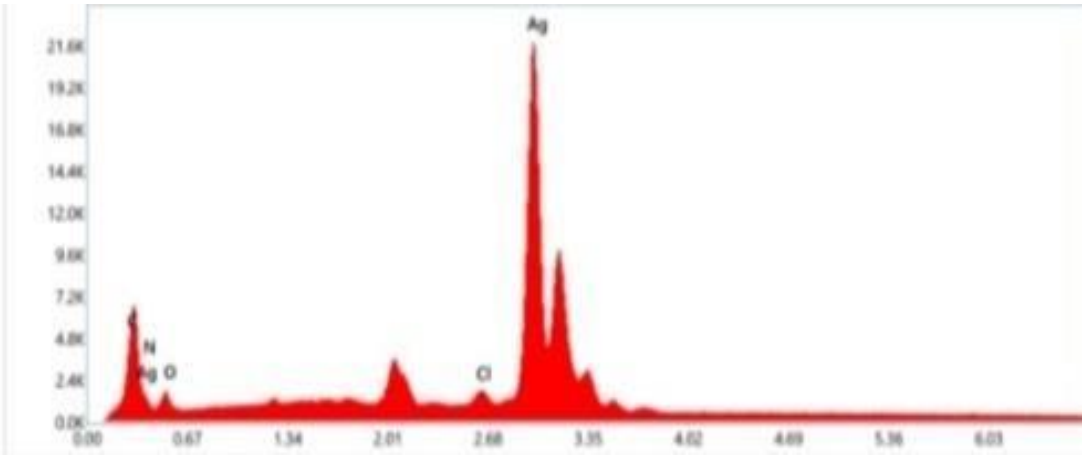

Figure 34: EDX spectrum of synthesized AgNPs by RC- root extract.

Table 11: Composition of different elements present in synthesized AgNPs RC-root.

Element	**Weight %**	**MDL**	**Atomic %**	**Net Int.**	**Error %**	**R**	**A**	**F**
C K	4.9	0.18	28.1	223.4	8.7	0.7230	0.4338	1.0000
N K	0.6	0.16	2.9	25.1	20.0	0.7324	0.2173	1.0000
O K	2.3	0.18	9.7	79.0	13.7	0.7405	0.1381	1.0000
Cl K	0.00	0.0	0.0	0.0	100.0	0.8148	0.8830	1.0719
Ag L	92.3	0.40	59.3	3063.2	3.7	0.8303	0.9143	1.0040

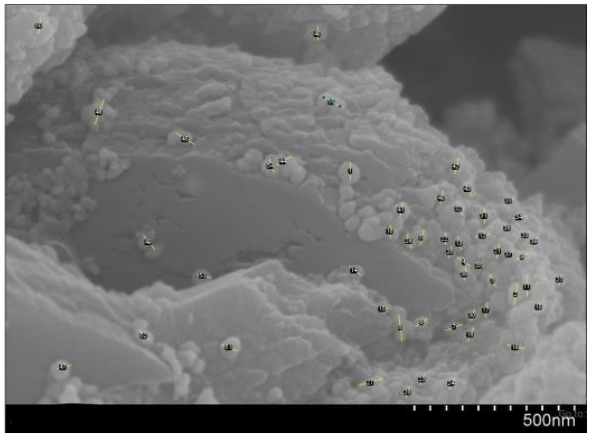

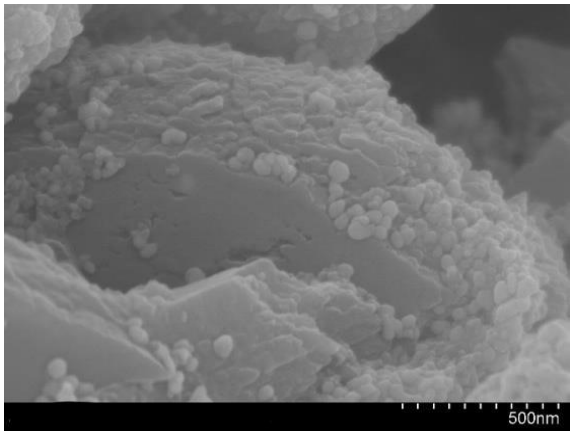

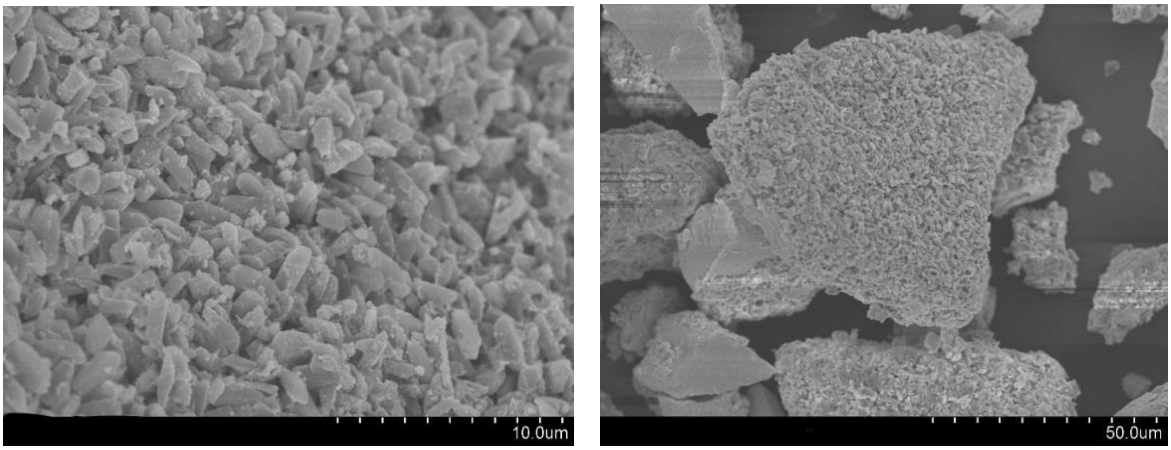

Figure 35: FE-SEM images of synthesized AgNPs RC- leaf extract.

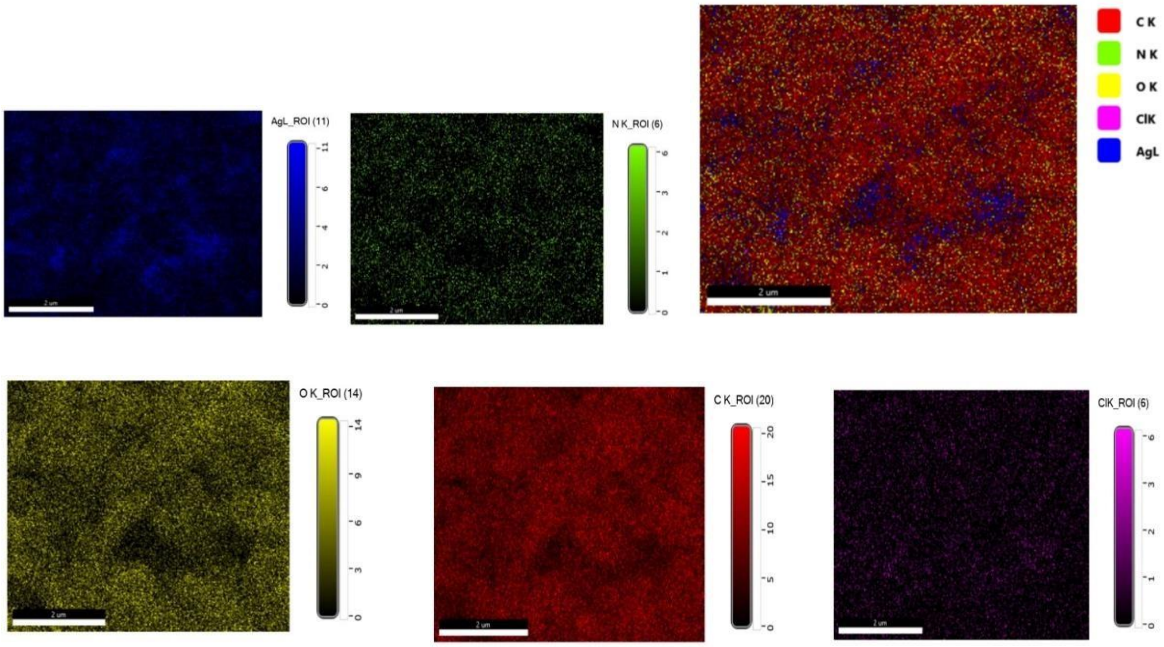

Figure 36: An energy-dispersive x-ray (EDX) spectrum of AgNPs with total elemental mapping and individual color mapping of synthesized AgNPs RC-leaf extract.

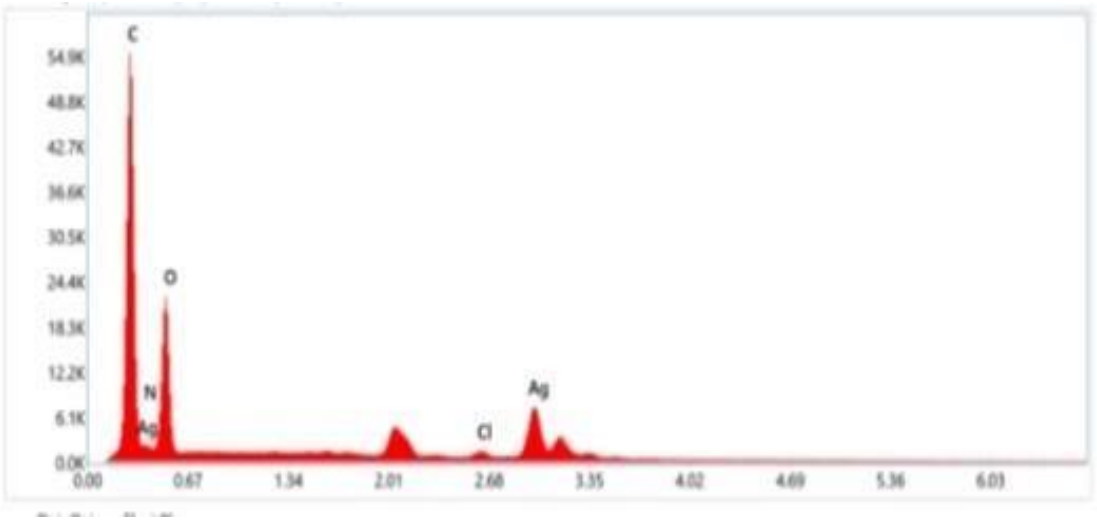

Figure 37: EDX spectrum of synthesized AgNPs by RC-leaf extract.

Table 12: Composition of different elements present in synthesized AgNPs RC-leaf.

Element	Weight %	MDL	Atomic %	Net Int.	Error %	R	A	F
C K	56.7	0.07	74.0	4245.7	7.2	0.9022	0.4757	1.0000
N K	1.9	0.20	2.1	73.1	18.2	0.9094	0.1306	1.0000
O K	21.3	0.13	20.8	1712.1	10.2	0.9151	0.2137	1.0000
Cl K	0.4	0.07	0.2	65.4	10.2	0.9547	0.9534	1.0466
Ag L	19.7	0.22	2.9	994.5	3.8	0.9607	0.9686	1.0042

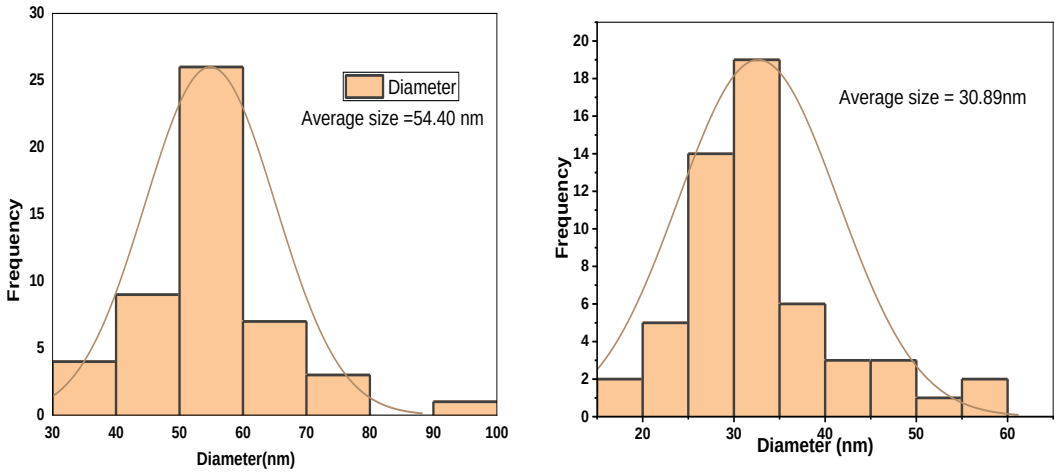

Figure 38: SEM images of the synthesized AgNPs RC- root and leaf extract showing particle size through a histogram.

4.8 Antimicrobial activity

Disk- diffusion method was used to determine the antimicrobial activity of plant extract and synthesized silver nanoparticles of RC-root and leaf. In such a study 1 mg/ml neomycin and distilled water were used as a positive and negative control.

Table 13. Antimicrobial screening of plant extracts along with its synthesized silver nanoparticles extracts

Extracts	**Name of bacteria**	**ZOI (mm)**	**ZOI of PC(neomycin)**
RLA		7.0 ± 0.0	18
RLS	*Staphylococcus*	7.5 ± 0.29	17
RRA	*aureus* ATCC	6.0 ± 0.0	18
RRS	43300	7.83 ± 0.17	17
RLA		5.67 ± 0.17	20
RLS	*Klebsiella*	7.0 ±0.29	20
RRA	*pneumonia*	5.0 ± 0.0	17
RRS	ATCC 700603	6.17 ± 0.17	20

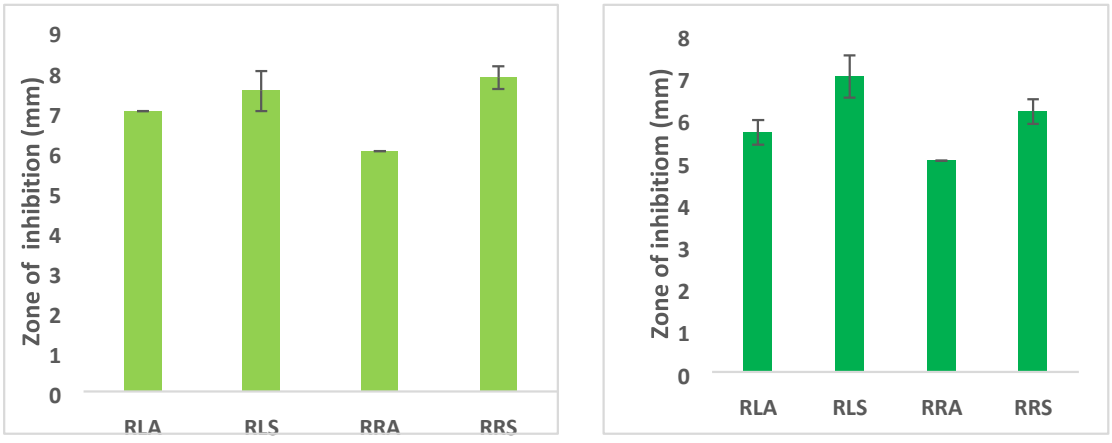

Figure 39: Comparative study of a zone of inhibition shown by plant extract and its silver nanoparticles against bacteria *Staphylococcus aureus* and *Klebsiella pneumonia*

Where R= *Rhus chinensis*, L=leaf, R= root A= aqueous S= silver nanoparticles

From Table 13 and the comparative study of ZOI, the obtained data showed that silver nanoparticles of both RC- root and leaf extract were active against bacteria

Staphylococcus aureus and *Klebsiella pneumonia* as compared to plant extract. Among them, the synthesized silver nanoparticle of RC-root extract was active against Gram-positive bacteria *Staphylococcus aureus* with ZOI values of 7.83 ± 0.17 whereas the synthesized silver nanoparticle of RC-leaf extract was active against Gram-negative bacteria *Klebsiella pneumonia* with ZOI values of 7.0 ±0.29.

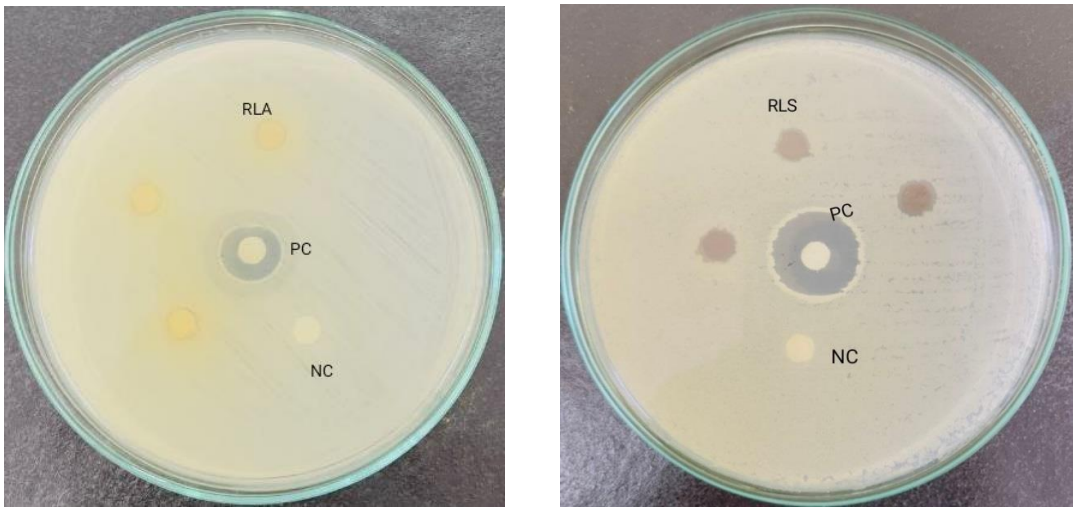

Figure 40: ZOI of plant extract along with its synthesized silver nanoparticles of RC-leaf extracts against bacteria *Staphylococcus aureus*

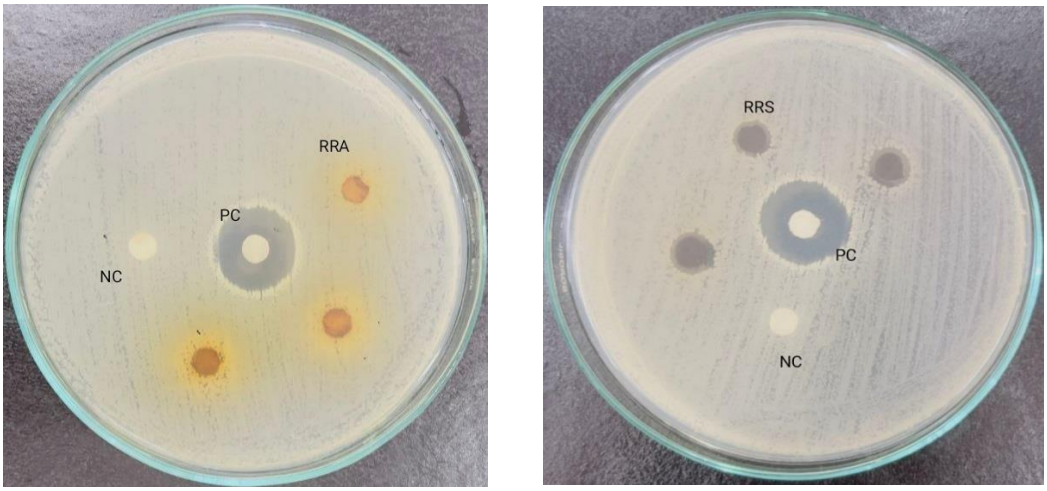

Figure 41: ZOI of plant extract along with its synthesized silver nanoparticles of RC-root extracts against bacteria *Staphylococcus aureus*

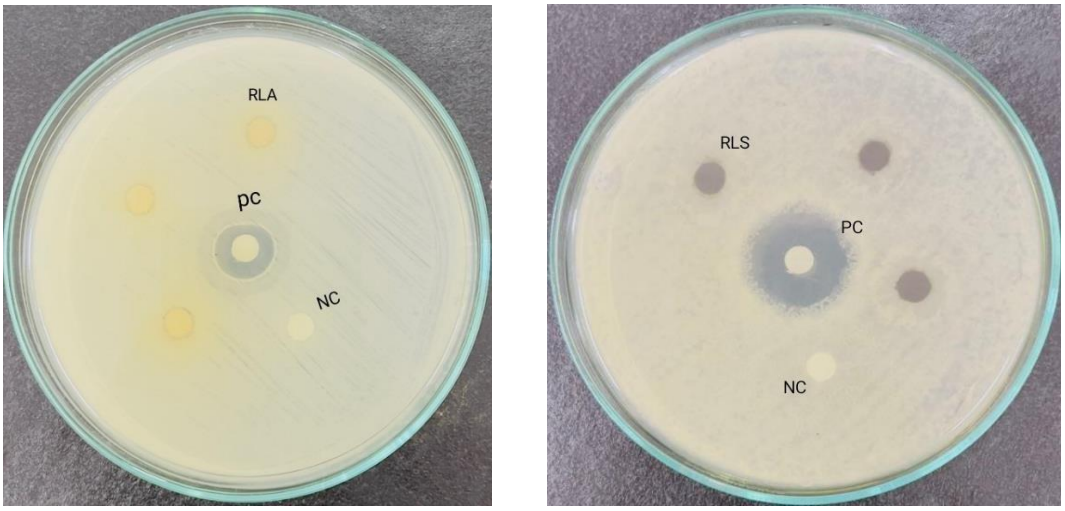

Figure 42: ZOI of plant extract along with its synthesized silver nanoparticles of RC-leaf extracts against bacteria *Klebsiella pneumonia*

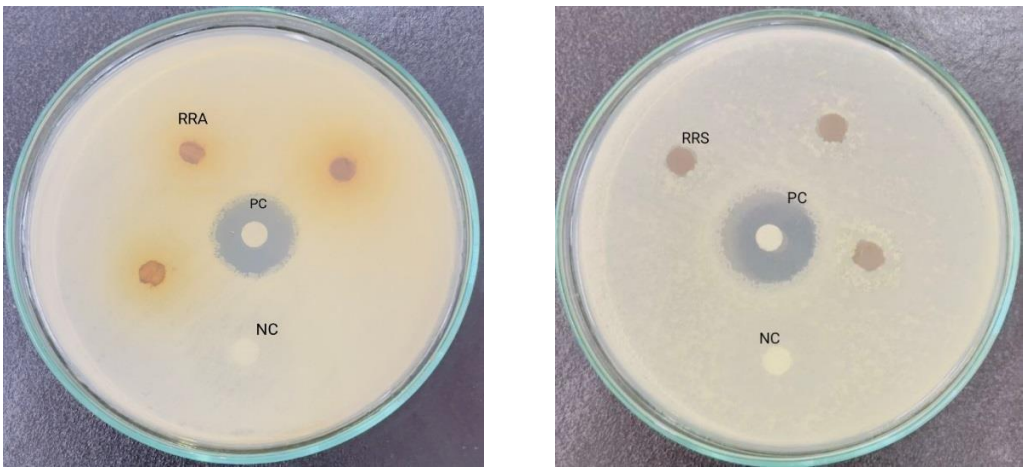

Figure 43: ZOI of plant extract along with its synthesized silver nanoparticles of RC-root extracts against bacteria *Klebsiella pneumonia*

Discussion

Rhus chinensis Mill is one of the popular traditional medicines with great potential for useful secondary metabolites. Many parts of the plant are used by local people for medicinal purposes. *Rhus chinensis* Mill leaves are being used to cure various health problems such as depurative, stimulation, blood circulation, hemoptysis, inflammations, laryngitis, stomachache, traumatic fractures, snake bite, diarrhea, and its fruits are used for colic, diarrhea, dysentery, jaundice, and hepatitis. A previous study reported that the TPC and TFC value of *Rhus chinensis* was 117.092 ± 1.1 mg GAE/g and 62.41 ± 1.23 mg QE/g of fruit-dried extract respectively (Dhakal et al.,

2022). In this study, the TPC and TFC value of *Rhus chinensis* of fruit dried extract was found to be 104.195 ± 0.425 mg GAE/g and 44.690 ± 0.958 mg QE/g but overall in this study root dried extract showed the highest TPC and TFC values of 141.480 ± 0.665 mg GAE/g and 54.345 ± 0.279 mg QE/g respectively. The values of TPC and TFC were almost different as compared to the standard given literature. Such difference in the value of TPC and TFC relies on the collection time, environmental factor altitude, extraction process, and extraction solvent. According to this same literature, 50% DPPH scavenging activity of crude extract of *Rhus chinensis* fruit was observed at 7.963 µg/mL. This study determined that 50% DPPH-free radical scavenging activity of crude extract fruit was found to be 10.117 ± 0.471 µg/mL. But in an overall investigation of this study crude extract of *Rhus chinensis* root was found to be more potent as compared to fruit 7.830 ± 0.187 µg/mL. Agar-well diffusion method was used to determine the antimicrobial activity of *Rhus chinensis*. This study investigated *Rhus chinensis* root was found effective against Gram-positive bacteria ATCC 43300 *Staphylococcus aureus* of ZOI 22 mm whereas, ZOI of positive control Neomycin was found to be 25mm. *Rhus chinensis* leaf extract was found effective against Gram-negative bacteria ATCC 2591 *Escherichia coli of* ZOI 25 mm respectively and the ZOI of positive control Neomycin for these bacteria was found to be 20 mm which was quite interesting because of the higher ZOI value of positive control than plant leaf extract. Higher phenolic and flavonoid content might have aided in the quick and simple reduction of silver ions and the stability of those ions. Silver nanoparticles were synthesized by various characterization techniques. In such a study characterization of the sample was done by UV- visible spectroscopy, XRD, FTIR, FE-SEM, and EDX. Visualization of color changing of nanoparticles from yellowish extract solution to reddish brown color investigated the formation of nanoparticles which was also matched with (Khanal et al., 2022). The synthesis of AgNPs RC-root and RC-leaf was tracked at different time intervals by the change of color and absorption spectra appeared at around 443 nm and 441 nm, respectively while the biosynthesized silver nanoparticles of *hibiscus rosasinensis* extract were discovered at about 400 -450 nm (Periasamy et al., 2022) which was matched to the literature. FTIR spectra are very useful for identifying the functional group present in the sample. As compared to the extract with synthesized silver nanoparticles of both RC-Root and RC-leaf extract the absorption peak is found to be almost the same but slight difference in the synthesized silver nanoparticle extract peak in case of intense peak. The absorption peak was found

for both synthesized AgNPs extract was found to be aromatic –CH stretching and bending, -OH stretching and bending, -C=C- stretching, -C-O, and C-N at 2987 $cm^{-1,}$ and 879 cm^{-1}, 3197 cm^{-1}, and 1394 cm^{-1}, 1608 cm^{-1}, 1242 cm^{-1} and 1066 cm^{-1} respectively. Previously reported the involvement of functional groups like N-H, C=O, and C-C in AgNP synthesis (Patil et al., 2016). This result showed that oxidized polyphenols have capped the surface RC-AgNPs. The average crystallite size of the synthesized RC-AgNPs of root and leaf extract was calculated by the Debye-Scherer formula and it was found to be 11.01 nm and 13.39 nm respectively. As compared to the literature (Giri & Sharma, 2022)the particle was found to slight difference of 6.1 nm. High-density synthesized AgNPs are shown by FE-SEM analysis. In this study, the SEM image of synthesized AgNPs RC-root extract was relatively found to be spherical and had no agglomeration with a diameter of 54.40 nm whereas synthesized

AgNPs RC-leaf extract was found to be spherical with a rod shape and a little bit of agglomeration with a diameter of 30.89nm. (Raghava et al., 2021) also examined that synthesized silver nanoparticles formed by *Rivina humilis* leaf extract were found to be spherical with a diameter of 51nm. The presence of silver components was confirmed by the EDX characterization technique or analysis. In this study, thorough EDX the peak of silver in both AgNPs root and leaf extract showed around 3kev, and other elements like Cl, O, C, and N were also reported with synthesized AgNPs which was matched with literature (Patil et al., 2016). The diameter of synthesized AgNPs was also shown with the help of a histogram graph. The synthesized silver nanoparticle of RC-root extract was active against Gram-positive bacteria *Staphylococcus aureus* with ZOI values of 7.83 ± 0.17 whereas the synthesized silver nanoparticle of RC-leaf extract was active against Gram-negative bacteria *Klebsiella pneumonia* with ZOI values of 7.0 ±0.29. This study revealed that silver nanoparticles showed activity against bacteria as compared to their plant extract.

CHAPTER 5

CONCLUSION AND RECOMMENDATION

5.1 Conclusion

Rhus chinensis could be rich sources of phytoconstituents. From the phytochemical analysis test, the phytochemicals present in fruits, leaves, bark, and root extract of *Rhus chinensis* were found to be; phenols, flavonoids, terpenoids, quinine, saponins, carbohydrates, tannins, and alkaloids. The comparative study of all these four parts of plant crude extract of *Rhus chinensis* root extract showed higher TPC, TFC, and antioxidant properties. The higher the phenolic content higher will be the antioxidant properties that is, the phenolic group is directly proportional to the antioxidant properties. Hence, this study proved that the higher the TPC, the TFC value more be the antioxidant activity. And there is also directly correlated with antimicrobial activity. The root part of *Rhus chinensis* showed effectiveness against Gram-positive bacteria *Staphylococcus aureus* ATCC 43300 and the leaf part showed effectiveness against Gram-negative activity bacteria *Escherichia coli* ATCC 25922. Adopting a green synthesis process to make silver nanoparticles is a quicker, more efficient, and less expensive method. Since the synthesis doesn't result in the creation of any hazardous chemicals. It has been demonstrated that an extract of the leaves and root of *R. chinensis* acts as a good reductant for the manufacture of colloidal silver nanoparticles process. On the other hand, the greenly synthesized silver nanoparticles, which were made from the root and leaves of *Rhus chinensis*, demonstrated their antibacterial effectiveness against several microbes. In contrast, the silver nanoparticles made from root extract demonstrated very effective microorganism suppression.

5.2 Recommendation

Further research to isolate, purify, describe, and standardize the bioactive constituents from the active extract of *Rhus chinensis* is strongly encouraged by the current study. It will be possible to conduct in vivo and in vitro activity tests on the selected plant extracts as part of the drug discovery process. To support the traditional therapeutic use of this plant in a way that is supported by science, more study and research is consequently needed. Additionally, it is advised to use contemporary computational systems for in silico molecular docking methodologies and computational approaches

to isolate bioactive molecules. Consequently, more research must be done to determine the plant's medical potential.

REFERENCES

A, A., & S, V. (2018). X-ray Diffraction (XRD) and Energy Dispersive Spectroscopy (EDS) Analysis of Silver Nanoparticles Synthesized from *Erythrina Indica* Flowers. *Nanoscience & Technology Open Access*, *5*(1). https://symbiosisonlinepublishing.com/nanoscience-technology/

Acharya, R. (2012). Ethnobotanical study of medicinal plants of Resunga hill used by Magar community of Badagaun VDC, Gulmi district, Nepal. *Scientific World*, *10*(10), Article 10. https://doi.org/10.3126/sw.v10i10.6863

Ahmad, S., Munir, S., Zeb, N., Ullah, A., Khan, B., Ali, J., Bilal, M., Omer, M., Alamzeb, M., Salman, S. M., & Ali, S. (2019). Green nanotechnology: A review on green synthesis of silver nanoparticles - an eco-friendly approach. *International Journal of Nanomedicine*, *14*, 5087–5107. https://doi.org/10.2147/IJN.S200254

Alam, N., & Sharma, K. (2020). Estimation of phenolic content, flavonoid content, antioxidant, and alpha-amylase inhibitory activity of some selected plants from Siraha district Nepal. *Asian Journal of Pharmaceutical and Clinical Research*, *13*, 28–35. https://doi.org/10.22159/ajpcr.2020.v13i4.36734

Al-Jaroudi, S. S., Ul-Hamid, A., Mohammed, A.-R. I., & Saner, S. (2007). Use of Xray powder diffraction for quantitative analysis of carbonate rock reservoir samples. *Powder Technology*, *175*(3), 115–121. https://doi.org/10.1016/j.powtec.2007.01.013

Anandalakshmi, K., Venugobal, J., & Ramasamy, V. (2016). Characterization of silver nanoparticles by green synthesis method using *Pedalium* murex leaf extract and their antibacterial activity. *Applied Nanoscience*, *6*(3), 399–408. https://doi.org/10.1007/s13204-015-0449-z

Arshad, M., Khan, A., Farooqi, Z. H., Usman, M., Waseem, M. A., Shah, S. A., & Khan, M. (2018). Green synthesis, characterization, and biological activities of silver nanoparticles using the bark extract of *Ailanthus altissima*. *Materials Science-Poland*, *36*(1), 21–26. https://doi.org/10.1515/msp-2017-0100

Ashraf, J. M., Ansari, M. A., Khan, H. M., Alzohairy, M. A., & Choi, I. (2016). Green synthesis of silver nanoparticles and characterization of their inhibitory effects on AGEs formation using biophysical techniques. *Scientific Reports*, *6*, 20414. https://doi.org/10.1038/srep20414

Ayoka, T. O., Ezema, B. O., Eze, C. N., & Nnadi, C. O. (2022). Antioxidants for the Prevention and Treatment of Non-communicable Diseases. *Journal of Exploratory Research in Pharmacology*, *7*(3), 178–188. https://doi.org/10.14218/JERP.2022.00028

Barani, M., Sangiovanni, E., Angarano, M., Rajizadeh, M. A., Mehrabani, M., Piazza, S., Gangadharappa, H. V., Pardakhty, A., Mehrbani, M., Dell'Agli, M., & Nematollahi, M. H. (2021). Phytosomes as Innovative Delivery Systems for Phytochemicals: A Comprehensive Review of Literature. *International Journal of Nanomedicine*, *16*, 6983–7022. https://doi.org/10.2147/IJN.S318416

Chandra, S., Khan, S., Avula, B., Lata, H., Yang, M. H., ElSohly, M. A., & Khan, I. A. (2014). Assessment of Total Phenolic and Flavonoid Content, Antioxidant Properties, and Yield of Aeroponically and Conventionally Grown Leafy Vegetables and Fruit Crops: A Comparative Study. *Evidence-Based Complementary and Alternative Medicine : ECAM*, *2014*, 253875. https://doi.org/10.1155/2014/253875

Chhetri, S. B. B., Khatri, D., & Parajuli, K. (2020). Antioxidant, Anti-Inflammatory, and Analgesic Activities of Aqueous Extract of *Diploknema butyracea* (Roxb.) H.J. Lam Bark. *The Scientific World Journal*, *2020*, e6141847. https://doi.org/10.1155/2020/6141847

Dhakal, K., Shrestha, D., Pokhrel, T., Panta, P., Pandey, A., Dhakal, J., & Adhikari, A. (2022). Antioxidant, Antibacterial, Antidiabetic Potential, and In Silico Analysis of *Rhus chinensis* from Western Nepal. *Current Topics in Medicinal Chemistry*, *22*. https://doi.org/10.2174/1568026622666220803153226

Djakpo, O., & Yao, W. (2010). *Rhus chinensis* and *Galla Chinensis* – folklore to modern evidence: Review. *Phytotherapy Research*, *24*(12), 1739–1747. https://doi.org/10.1002/ptr.3215

Ghasemzadeh, A., Jaafar, H. Z. E., & Rahmat, A. (2010). Antioxidant Activities, Total Phenolics and Flavonoids Content in Two Varieties of Malaysia Young Ginger (*Zingiber officinale* Roscoe). *Molecules*, *15*(6), 4324–4333. https://doi.org/10.3390/molecules15064324

Giri, R., & Sharma, K. (2022). Biogenic Synthesis of Silver Nanoparticles Using *Terminalia chebula* Retz. Leaf Extract and Evaluation of Biological Activities. *Journal of Nepal Chemical Society*, *43*(1), Article 1. https://doi.org/10.3126/jncs.v43i1.46957

Hussein, H. A., & Abdullah, M. A. (2020). Biosynthesis, Mechanisms, and Biomedical Applications of Silver Nanoparticles. In D. Thangadurai, J. Sangeetha, & R. Prasad (Eds.), *Functional Bionanomaterials: From Biomolecules to Nanoparticles* (pp. 313–332). Springer International Publishing. https://doi.org/10.1007/978-3-030-41464-1_14

Iwu, M., Duncan, A., & Okunji, C. (1999). New Antimicrobials of Plant Origin. *Perspectives on New Crops and New Uses*.

Jalab, J., Abdelwahed, W., Kitaz, A., & Al-Kayali, R. (2021). Green synthesis of silver nanoparticles using aqueous extract of *Acacia* cyanophyte and its antibacterial activity. *Heliyon*, *7*(9), e08033. https://doi.org/10.1016/j.heliyon.2021.e08033

Jones, W. P., & Kinghorn, A. D. (2012). Extraction of plant secondary metabolites. *Methods in Molecular Biology (Clifton, N.J.)*, *864*, 341–366. https://doi.org/10.1007/978-1-61779-624-1_13

Joshi, B., Panda, S. K., Jouneghani, R. S., Liu, M., Parajuli, N., Leyssen, P., Neyts, J., & Luyten, W. (2020). Antibacterial, Antifungal, Antiviral, and Anthelmintic Activities of Medicinal Plants of Nepal Selected Based on Ethnobotanical Evidence. *Evidence-Based Complementary and Alternative Medicine: ECAM*, *2020*, 1043471. https://doi.org/10.1155/2020/1043471

Kalita, S., Kumar, G., Karthik, L., & Rao, K. V. B. (2011). *Phytochemical Composition and In Vitro Hemolytic Activity of Lantana Camara L. (Verbenaceae) Leaves*.

Karki, R., Talchabhadel, R., Aalto, J., & Baidya, S. K. (2016). New climatic classification of Nepal. *Theoretical and Applied Climatology*, *125*(3), 799–808. https://doi.org/10.1007/s00704-015-1549-0

Khan, S. A., Shahid, S., Shahid, B., Fatima, U., & Abbasi, S. A. (2020). Green Synthesis of MnO Nanoparticles Using *Abutilon indicum* Leaf Extract for Biological, Photocatalytic, and Adsorption Activities. *Biomolecules*, *10*(5), 785. https://doi.org/10.3390/biom10050785

Khanal, L. N., Sharma, K. R., Paudyal, H., Parajuli, K., Dahal, B., Ganga, G. C., Pokharel, Y. R., & Kalauni, S. K. (2022). Green Synthesis of Silver Nanoparticles from Root Extracts of *Rubus ellipticus* Sm. And Comparison of Antioxidant and Antibacterial Activity. *Journal of Nanomaterials*, *2022*, e1832587. https://doi.org/10.1155/2022/1832587

Kupina, S., Fields, C., Roman, M. C., & Brunelle, S. L. (2018). Determination of Total Phenolic Content Using the Folin-C Assay: Single-Laboratory Validation, First Action 2017.13. *Journal of AOAC INTERNATIONAL*, *101*(5), 1466–1472. https://doi.org/10.5740/jaoacint.18-0031

Li.-R., Xie, X.-B., Shi, Q.-S., Zeng, H.-Y., OU-Yang, Y.-S., & Chen, Y.-B. (2010). Antibacterial activity and mechanism of silver nanoparticles on Escherichia coli. *Applied Microbiology and Biotechnology*, *85*(4), 1115–1122. https://doi.org/10.1007/s00253-009-2159-5

Link, S., & El-Sayed, M. A. (2003). Optical properties and ultrafast dynamics of metallic nanocrystals. *Annual Review of Physical Chemistry*, *54*, 331–366. https://doi.org/10.1146/annurev.physchem.54.011002.103759

Locatelli, M., Gindro, R., Travaglia, F., Coïsson, J.-D., Rinaldi, M., & Arlorio, M. (2009). Study of the DPPH-scavenging activity: Development of free software for the correct interpretation of data. *Food Chemistry*, *114*(3), 889–897. https://doi.org/10.1016/j.foodchem.2008.10.035

Melkamu, W. W., & Bitew, L. T. (2021). Green synthesis of silver nanoparticles using *Hagenia abyssinica* (Bruce) J.F. Gmel plant leaf extract and their antibacterial and antioxidant activities. *Heliyon*, *7*(11), e08459.

https://doi.org/10.1016/j.heliyon.2021.e08459

Mikhailova, E. O. (2020). Silver Nanoparticles: Mechanism of Action and Probable Bio-Application. *Journal of Functional Biomaterials*, *11*(4), 84. https://doi.org/10.3390/jfb11040084

Miksicek, R. J. (1993). Commonly occurring plant flavonoids have estrogenic activity. *Molecular Pharmacology*, *44*(1), 37–43.

Molyneux, R. J., Lee, S. T., Gardner, D. R., Panter, K. E., & James, L. F. (2007). Phytochemicals: The Good, the Bad, and the Ugly? *Phytochemistry*, *68*(22–24), 2973–2985. https://doi.org/10.1016/j.phytochem.2007.09.004

Muflihah, Y. M., Gollavelli, G., & Ling, Y.-C. (2021). Correlation Study of Antioxidant. Activity with Phenolic and Flavonoid Compounds in 12 Indonesian Indigenous Herbs. *Antioxidants*, *10*(10), 1530. https://doi.org/10.3390/antiox10101530

Mwankuna, C. J., Mariki, E. E., Mabiki, F. P., Malebo, H. M., Styrishave, B., & Mdegela, R. H. (2023). Thin Layer Chromatographic Method for Detection of Conventional Drug Adulterants in Herbal Products. *Separations*, *10*(1), Article 1. https://doi.org/10.3390/separations10010023

Nieto, G., Ros, G., & Castillo, J. (2018). Antioxidant and Antimicrobial Properties of Rosemary (*Rosmarinus officinalis*, L.): A Review. *Medicines (Basel, Switzerland)*, *5*(3), 98. https://doi.org/10.3390/medicines5030098

Panthi, M., & Singh, A. (2013). Ethnobotany of Arghakhanchi District, Nepal: Plants used in dermatological and cosmetic disorders. *International Journal of Applied Sciences and Biotechnology*, *1*. https://doi.org/10.3126/ijasbt.v1i2.8199

Patil, M. P., Rokade, A. A., Ngabire, D., & Kim, G.-D. (2016). Green Synthesis of Silver Nanoparticles Using Water Extract from Galls of *Rhus Chinensis* and Its Antibacterial Activity. *Journal of Cluster Science*, *27*(5), 1737–1750. https://doi.org/10.1007/s10876-016-1037-4

Periasamy, S., Jegadeesan, U., Sundaramoorthi, K., Rajeswari, T., Tokala, V. N. B., Bhattacharya, S., Muthusamy, S., Sankoh, M., & Nellore, M. K. (2022). Comparative Analysis of Synthesis and Characterization of Silver

Nanoparticles Extracted Using Leaf, Flower, and Bark of *Hibiscus Rosa sinensis* and Examine Its Antimicrobicidal Activity. *Journal of Nanomaterials*, *2022*, e8123854. https://doi.org/10.1155/2022/8123854

Pham-Huy, L. A., He, H., & Pham-Huy, C. (2008). Free Radicals, Antioxidants in Disease and Health. *International Journal of Biomedical Science : IJBS*, *4*(2), 89–96.

Raghava, S., Munnene Mbae, K., & Umesha, S. (2021). Green synthesis of silver nanoparticles by *Rivina humilis* leaf extract to tackle the growth of Brucella species and other perilous pathogens. *Saudi Journal of Biological Sciences*, *28*(1), 495–503. https://doi.org/10.1016/j.sjbs.2020.10.034

Rahman, Md. M., Islam, Md. B., Biswas, M., & Khurshid Alam, A. H. M. (2015). In vitro antioxidant and free radical scavenging activity of different parts of *Tabebuia pallida* growing in Bangladesh. *BMC Research Notes*, *8*(1), 621. https://doi.org/10.1186/s13104-015-1618-6

Rautela, A., Rani, J., & Debnath (Das), M. (2019). Green synthesis of silver nanoparticles from *Tectona grandis* seeds extracts Characterization and mechanism of antimicrobial action on different microorganisms. *Journal of Analytical Science and Technology*, *10*(1), 5. https://doi.org/10.1186/s40543018-0163-z

Ren, Z., Zhu, B., Wang, D., Ma, E., Su, D., & Zhong, Y. (2008). Comparative population structure of Chinese sumac aphid *Schlechtendalia chinensis* and its primary host-plant *Rhus chinensis*. *Genetica*, *132*(1), 103–112. https://doi.org/10.1007/s10709-007-9153-6

Sariozlu, N. Y., & Kivanc, M. (2011). Chapter 60—Gallnuts (Quercus infectoria Oliv. And *Rhus chinensis* Mill.) and Their Usage in Health. In V. R. Preedy, R. R. Watson, & V. B. Patel (Eds.), *Nuts and Seeds in Health and Disease Prevention* (pp. 505–511). Academic Press. https://doi.org/10.1016/B978-0-12-375688-6.10060-X

Sharifi-Rad, M., Anil Kumar, N. V., Zucca, P., Varoni, E. M., Dini, L., Panzarini, E., Rajkovic, J., Tsouh Fokou, P. V., Azzini, E., Peluso, I., Prakash Mishra, A., Nigam, M., El Rayess, Y., Beyrouthy, M. E., Polito, L., Iriti, M., Martins, N.,

Martorell, M., Docea, A. O., Sharifi-Rad, J. (2020). Lifestyle, Oxidative Stress, and Antioxidants: Back and Forth in the Pathophysiology of Chronic Diseases. *Frontiers in Physiology*, *11*. https://www.frontiersin.org/articles/10.3389/fphys.2020.00694

Sharma, K. R., Kalauni, S. K., & Awale, S. (2015). Antioxidant, Phytotoxic and Antimicrobial Activities of Methanolic Extract of *Bauhinia* variegata Barks. *Journal of Institute of Science and Technology*, *20*(2), Article 2. https://doi.org/10.3126/jist.v20i2.13946

Sharma, T., Pandey, B., Shrestha, B. K., Koju, G. M., Thusa, R., & Karki, N. (2020). Phytochemical Screening of Medicinal Plants and Study of the Effect of Phytoconstituents in Seed Germination. *Tribhuvan University Journal*, *35*(2), Article 2. https://doi.org/10.3126/tuj.v35i2.36183

Shi, L., Zheng, L., Liu, R., Chang, M., Huang, J., Zhao, C., Jin, Q., & Wang, X. (2019). Potentially underutilized oil resources from the fruit and seed of *Rhuchinensis Mill*. Industrial Crops and Products, *129*, 339–344. https://doi.org/10.1016/j.indcrop.2018.12.023

Sulaiman, C. T., & Balachandran, I. (2012). Total phenolics and total flavonoids in selected Indian medicinal plants. *Indian Journal of Pharmaceutical Sciences*, *74*(3), 258–260. https://doi.org/10.4103/0250-474X.106069

Tian, F., Li, B., Ji, B., Yang, J., Zhang, G., Chen, Y., & Luo, Y. (2009). Antioxidant and antimicrobial activities of consecutive extracts from Galla *chinensis:* The polarity affects the bioactivities. *Food Chemistry*, *113*(1), 173–179. https://doi.org/10.1016/j.foodchem.2008.07.062

Wuttisin, N., & Boonsook, W. (2019). Total Phenolic, Flavonoid Contents and Antioxidant Activity of *Siraitia* grosvenorii Fruits Extracts. *Food and Applied Bioscience Journal*, *7*(3), Article 3.

Y., Zhao, L., Cai, S., & Cheng, G. (2018). Acute and subchronic toxicities of the ethanol and hot-water extracts from Chinese sumac (*Rhus chinensis* Mill.) fruits by oral administration in rats. *Food and Chemical Toxicology*, *119*, 14–23. https://doi.org/10.1016/j.fct.2018.06.009

Zhang, C., Ma, Y., Gao, F., Zhao, Y., Cai, S., & Pang, M. (2018). The free, esterified, and insoluble-bound phenolic profiles of *Rhus chinensis* Mill. Fruits and their pancreatic lipase inhibitory activities with molecular docking analysis. *Journal of Functional Foods*, *40*, 729–735. https://doi.org/10.1016/j.jff.2017.12.019

Zhang, C., Ma, Y., Zhao, Y., Hong, Y., Cai, S., & Pang, M. (2018). Phenolic composition, antioxidant and pancreatic lipase inhibitory activities of Chinese sumac (*Rhus chinensis* Mill.) fruits extracted by different solvents and interaction between myricetin-3-O-rhamnoside and quercetin-3-O-rhamnoside. *International Journal of Food Science & Technology*, *53*(4), 1045–1053. https://doi.org/10.1111/ijfs.13680

Zhang, X.-F., Liu, Z.-G., Shen, W., & Gurunathan, S. (2016). Silver Nanoparticles: Synthesis, Characterization, Properties, Applications, and Therapeutic Approaches. *International Journal of Molecular Sciences*, *17*(9), 1534. https://doi.org/10.3390/ijms17091534

Zheng, J., Nagashima, K., Parmiter, D., de la Cruz, J., & Patri, A. K. (2011). SEM Xray microanalysis of nanoparticles present in tissue or cultured cell thin sections. *Methods in Molecular Biology (Clifton, N.J.)*, *697*, 93–99. https://doi.org/10.1007/978-1-60327-198-1_9

APPENDIX-1

Phytochemical analysis (Kalita et al., 2011) and (T. Sharma et al., 2020)

1. Test for polyphenol

A dark green color, indicating the presence of phenolic chemicals, was achieved by adding two or three drops of 5% ferric chloride solution to the little amount of sample extract.

2. Test for tannins

Two or three drops of 0.1% ferric chloride solution were added to the sample extract.

Brownish green was obtained which indicates the presence of tannins.

3. Test for flavonoids

To a portion of filtrate, 10 mL of ethyl acetate and 2 mL of dil. The ammonia solution was kept and shaken well yellow coloration was present which indicates the presence of flavonoids.

4. Test for saponin

A few portions of dried sample crude extract were added to distilled water and shaken vigorously, foam was formed which indicates the presence of saponins

5. Test for volatile oils

A little amount of diluted HCL and 0.1 mL of NaOH were added to 2 mL of the extracted white ppt, indicating the presence of volatile oils

6. Test for carbohydrate/ glycosides

To the extract, con H_2SO_4 was added drop by drop then 5 ml of Molisch's reagent (methanol (50mL) was used to dissolve α-Napthol (5g)) was added and a discovery of a purple color ring at the junction of two liquids, indicates as a present of carbohydrates and glycosides.

7. Test for alkaloids

To the extract, Wagner's reagent (2 g iodine + 6 g KI in 100 mL distilled water) was kept, and a reddish brown ppt was involved which indicates the presence of alkaloids.

8. Test for glycosides

To the sample extract 3mL of chloroform, con HCl and 10% ammonium solution was added and shaken well it properly pink color was observed which indicates the presence of glycosides.

9. Test for Quinin

To the extract, freshly prepared $feso_4$ and ammonium thiocyanate were added and then con H_2SO_4 was added drop by drop. The deep red color was present which indicates the presence of quinine.

10. Test for terpenoids

Each sample was combined with 3 mL of con H_2SO_4 and 2 mL of chloroform, totaling 0.2 g. The presence of terpenoids is indicated by reddish-brown coloring.

APPENDIX-2

2.1 Determination of total phenolic content.

Absorbance at 765 nm for calibration curve of gallic acid at different concentrations measured in 96 well plates.

Concentration	Absorbance			Average	SD	SEM
10	0.055	0.045	0.061	0.054	0.008	0.005
20	0.096	0.111	0.105	0.104	0.008	0.004
30	0.134	0.142	0.14	0.139	0.004	0.002
40	0.18	0.17	0.165	0.172	0.008	0.004
50	0.207	0.208	0.191	0.202	0.010	0.006
60	0.228	0.25	0.27	0.249	0.021	0.012
70	0.306	0.251	0.289	0.282	0.028	0.016
80	0.32	0.307	0.316	0.314	0.007	0.004

Absorbance at 765 nm for calibration curve of plant extract at different concentrations measured in 96 well plates.

Plant extract	Absorbance			Concentration			TPC 1	TPC 2	TPC 3	Average	SD	SE
RLA	0.70	0.65	0.69	169.76	157.56	168.05	33.95	31.51	33.61	33.02	1.32	0.760
RLM	2.69	2.68	2.76	654.88	653.17	671.95	130.98	130.68	134.39	132.00	2.08	1.20
RLE	0.34	0.30	0.29	81.95	72.93	70.98	16.39	14.59	14.20	15.06	1.17	0.68
RLD	0.14	0.11	0.18	33.41	27.32	43.17	6.68	5.46	8.63	6.93	1.60	0.92
RLH	0.09	0.17	0.13	20.98	40.73	30.98	4.20	8.15	6.20	6.18	1.98	1.14
RBA	1.46	1.52	1.52	355.12	370.49	371.46	71.02	74.10	74.29	73.14	1.83	1.06
RBM	2.90	2.82	2.72	706.59	687.56	663.17	141.32	137.51	132.63	137.15	4.35	2.51
RBE	2.36	2.36	2.34	574.88	574.39	571.71	114.98	114.88	114.34	114.73	0.34	0.20

RBD	0.31	0.26	0.22	75.12	63.17	52.44	15.02	12.63	10.49	12.72	2.27	1.31
RBH	0.06	0.09	0.03	15.12	21.95	6.59	3.02	4.39	1.32	2.91	1.54	0.89
RFA	0.40	0.38	0.36	96.59	92.93	87.80	19.32	18.59	17.56	18.49	0.88	0.51
RFM	2.15	2.14	2.12	524.39	521.46	517.07	104.88	104.29	103.41	104.20	0.74	0.43
RFE	1.99	1.91	1.98	484.88	466.59	482.20	96.98	93.32	96.44	95.58	1.98	1.14
RFD	0.09	0.11	0.07	22.20	27.56	17.80	4.44	5.51	3.56	4.50	0.98	0.56
RFH	0.08	0.07	0.07	19.02	16.10	16.10	3.80	3.22	3.22	3.41	0.34	0.20
RRA	2.89	2.87	2.76	704.63	700.49	673.66	140.93	140.10	134.73	138.59	3.36	1.94
RRM	2.89	2.93	2.88	705.37	713.70	702.93	141.07	142.78	140.59	141.48	1.15	0.67
RRE	2.68	2.70	2.69	652.68	657.32	656.34	130.54	131.27	131.27	131.09	0.49	0.28
RRD	0.42	0.39	0.31	101.71	94.88	75.85	20.34	15.17	15.17	18.16	2.68	1.55
RRH	0.12	0.13	0.17	28.54	30.49	40.98	5.71	6.10	8.20	6.67	1.34	0.77

2.2 Determination of total flavonoid content.

Absorbance at 415 nm for calibration curve of quercetin acid at different concentrations measured in 96 well plates.

Concentration	Absorbance			Average	SD	SE
10	0.053	0.050	0.052	0.052	0.002	0.001
20	0.062	0.081	0.080	0.074	0.011	0.006
30	0.080	0.077	0.095	0.084	0.010	0.006
40	0.113	0.108	0.122	0.114	0.007	0.004
50	0.119	0.129	0.131	0.126	0.006	0.004
60	0.163	0.209	0.146	0.173	0.033	0.019
70	0.226	0.197	0.180	0.201	0.023	0.013
80	0.213	0.261	0.204	0.226	0.031	0.018
90	0.289	0.265	0.239	0.264	0.025	0.014
100	0.281	0.290	0.277	0.283	0.007	0.004

Absorbance at 415 nm for calibration curve of plant extract at different concentrations measured in 96 well plates.

Plant extract	Absorbance			Concentration			TFC 1	TFC 2	TFC 3	Average	SD	SE
RLA	0.12	0.13	0.13	42.41	43.10	45.86	8.48	8.62	9.17	8.76	0.36	0.21
RLM	0.57	0.58	0.58	195.17	200.34	198.62	39.03	40.07	39.72	39.61	0.53	0.30
RLE	0.55	0.46	0.48	187.93	157.59	165.52	37.59	31.52	33.10	34.07	3.15	1.82
RLD	0.28	0.28	0.30	97.24	95.17	104.83	19.45	19.03	20.97	19.82	1.02	0.59
RLH	0.11	0.10	0.18	37.24	35.86	61.72	7.45	7.17	12.34	8.99	2.91	1.68
RBA	0.07	0.08	0.07	24.48	27.59	24.48	4.90	5.52	4.90	5.10	0.36	0.21
RBM	0.10	0.12	0.14	34.48	42.41	49.66	6.90	8.48	9.93	8.44	1.52	0.88
RBE	0.69	0.69	0.68	237.24	237.59	234.83	47.45	47.52	46.97	47.31	0.30	0.17
RBD	0.60	0.61	0.58	206.55	211.38	198.62	41.31	42.28	39.72	41.10	1.29	0.74
RBH	0.12	0.17	0.16	41.38	58.28	56.55	8.28	11.66	11.31	10.41	1.86	1.07
RFA	0.02	0.04	0.04	6.55	14.48	14.14	1.31	2.90	2.83	2.34	0.90	0.52
RFM	0.65	0.67	0.62	224.14	231.38	214.83	44.83	46.28	42.97	44.69	1.66	0.96
RFE	0.35	0.43	0.36	121.38	149.31	123.10	24.28	29.86	24.97	26.25	3.13	1.81
RFD	0.22	0.29	0.21	76.21	98.28	72.07	15.24	19.66	14.41	16.44	2.82	1.63
RFH	0.19	0.23	0.18	66.21	80.00	61.72	13.24	16.00	12.34	13.86	1.90	1.10
RRA	0.44	0.40	0.43	150.34	137.59	148.97	30.07	27.52	29.79	29.13	1.40	0.81
RRM	0.06	0.07	0.07	21.38	22.41	24.48	4.28	4.48	4.90	4.55	0.32	0.18
RRE	0.80	0.78	0.79	274.14	269.31	271.72	54.83	53.86	54.34	54.34	0.48	0.28
RRD	0.41	0.42	0.41	139.66	143.45	142.07	27.93	28.69	28.41	28.34	0.38	0.22
RRH	0.65	0.65	0.65	225.17	224.14	222.76	45.03	44.83	44.55	44.80	0.24	0.14

2.3 DPPH free radical scavenging activity

Absorbance at 517nm for calibration curve of quercetin at different concentrations measured in 96 well plates.

Concentration	% Inhibition			Average	SD	SEM
10	67.80	68.12	75.13	70.35	4.14	2.39
5	65.24	64.28	66.57	65.36	1.15	0.66
2.5	45.16	70.67	43.25	53.03	15.31	8.84
1.25	34.24	35.89	35.23	35.12	0.83	0.48
0.06	7.23	12.01	12.96	10.73	3.07	1.78
0.03	8.50	3.40	4.68	5.53	2.65	1.73

Calculation of IC_{50} value of various plant extracts and quercetin

Plant extract	Half-maximal inhibitor concentration (IC_{50})			Average	SD	SE
RLH	49.45	49.60	47.23	48.76	1.32	0.76
RFH	408.14	408.14	408.64	408.15	0.51	0.29
RBH	71.75	65.8	62.9	66.817	4.51	2.60
RRH	47.62	45.58	38.50	43.90	4.78	2.76
RLD	73.95	72	70.25	72.06	1.85	1.06
RFD	69.64	68.77	68.79	69.93	0.50	0.28
RBD	42.20	43.35	43.30	42.95	0.64	0.37
RRD	68.55	69.1	70.85	69.50	1.20	0.69
RLE	83.4	77.6	78.25	79.75	3.17	1.83
RFE	72.15	68.85	68.8	69.93	1.92	1.10
RBE	7.82	8.16	9.06	8.34	0.64	0.37
RRE	8.19	7.72	7.57	7.83	0.32	0.18
RLM	49.77	49.28	44.57	47.87	2.87	1.65

RFM	12.35	13.69	13.39	13.14	0.70	0.40
RBM	61.2	62.95	60.05	61.40	1.46	0.84
RRM	58.7	55.55	56.2	56.81	1.66	0.96
RLA	23.86	24.52	22.55	23.64	1.00	0.58
RFA	11.03	9.86	9.46	10.11	0.81	0.47
RBA	18.76	21.53	16.83	19.04	2.36	1.36
RRA	33.64	34.79	34.26	34.23	0.57	0.33
QUERCETIN	2.61	1.66	2.49	2.25	0.51	0.29

2.4 Antimicrobial activity

Zone of inhibition of plant extracts to the various species of gram-positive and gramnegative bacteria.

Plant extracts	Names of bacteria	Diameter of ZOI of the sample(mm)	ZOI of the positive control Neomycin(mm)
RLE	*Shigella sonnei* ATCC 25931	15	25
	Staphylococcus aureus ATCC 43300	15	25
	Klebsiella pneumonia ATCC 700603	19	30
	Escherichia coli ATCC 25922	25	20
RBE	*Shigella sonnei* ATCC 25931	15	25
	Staphylococcus aureus ATCC 43300	16	25
	Klebsiella pneumonia ATCC 700603	15	30
	Escherichia coli ATCC 25922	14	20
RFE	*Shigella sonnei* ATCC 25931	12	25
	Staphylococcus aureus ATCC 43300	10	25
	Klebsiella pneumonia ATCC 700603	12	30
	Escherichia coli ATCC 25922	12	20
RRE	*Shigella sonnei* ATCC 25931	20	25
	Staphylococcus aureus ATCC 43300	22	25
	Klebsiella pneumonia ATCC 700603	18	30
	Escherichia coli ATCC 25922	-	20

2.4 Calculation of particle size from XRD of synthesized AgNPs RC-root and RC- leaf extract.

Two theta (2θ)	FWHM	Diameter (nm)	Average size particle (nm)
38.16	0.78	10.78	11.01
44.28	0.91	9.53	
64.51	0.79	11.89	
77.41	0.86	11.84	

Two theta (2θ)	FWHM	Diameter (nm)	Average size particle (nm)
38.20	0.59	14.25	13.39
44.28	0.73	11.75	
64.55	0.62	15.15	
77.44	0.82	12.42	

2.5 Calculation of particle size from FE-SEM of synthesized AgNPs RC-root and RC- leaf extract.

SN	Area	Standard deviation	Angle	Length
1	58	9.83	-60.75	57.30
2	46	2.55	63.43	44.72
3	66	7.67	21.80	64.62
4	54	5.38	12.99	53.36
5	51	2.65	-36.87	50
6	92	3.95	-46.79	90.55
7	63	9.41	-14.93	62.09
8	56	4.12	-66.25	54.62
9	50	4.66	-75.96	49.47
10	55	3.67	-51.00	54.03
11	55	11.17	-6.34	54.33
12	55	11.16	-74.93	53.85
13	53	3.60	87.79	52.03
14	54	2.03	-37.30	52.80
15	66	5.18	-16.18	64.56
16	52	5.06	-20.55	51.26

17	58	3.97	129.28	56.85
18	72	6.33	-81.87	70.71
19	59	4.52	-95.90	58.31
20	57	6.22	-106.50	56.32
21	65	9.85	77.27	63.56
22	50	3.99	-109.17	48.70
23	59	2.70	51.95	58.41
24	32	4.40	-63.43	31.30
25	69	4.09	90	68
26	57	3.93	-37.69	55.60
27	55	8.72	87.87	54.03
28	55	6.93	90	54
29	49	2.17	-112.24	47.53
30	53	3.83	-87.79	52.03
31	52	2.70	-141.34	51.22
32	47	2.32	49.39	46.09
33	60	10.57	-146.04	59.07
34	50	4.53	-123.36	49.09
35	55	10.13	151.04	53.71
36	51	2.78	-103.76	50.44
37	52	3.45	-78.69	50.99
38	50	1.75	-55.01	48.82
39	53	2.69	-35.53	51.61
40	77	4.27	-142.52	75.60
41	40	2.12	-124.50	38.83
42	50	4.42	78.23	49.03
43	74	5.35	-78.99	73.34
44	57	2.50	-76.11	56.32
45	54	6.53	34.28	53.25
46	43	4.27	-98.13	42.42
47	71	6.12	-76.75	69.85
48	39	5.70	-122.01	37.73
49	39	2.01	-86.98	38.05
50	62	8.60	70.97	61.35

SN	Area	Standard deviation	Angle	Length
1	41	5.00	-90	40
2	47	3.50	-100.08	45.70
3	31	5.02	-64.29	29.96
4	34	6.45	-32.73	33.28
5	31	7.16	-103.57	29.83
6	33	5.98	-145.30	31.62
7	36	3.22	21.50	35.46
8	57	6.30	-82.87	56.43
9	31	5.63	-152.59	30.41
10	21	3.30	-90	20
11	49	7.10	-87.61	48.04
12	35	4.69	-166.37	33.95
13	29	4.03	-79.87	28.44
14	34	5.91	-37.56	32.80
15	21	6.98	180	20
16	31	5.22	-90	30
17	35	5.40	-96.71	34.23
18	36	3.01	-113.62	34.92
19	41	3.30	168.40	39.81
20	21	9.33	-130.91	19.84
21	34	3.82	-100.62	32.55
22	27	7.69	-90	26
23	27	6.63	-114.62	26.40
24	27	7.58	-112.62	26
25	27	4.42	-112.62	26
26	28	3.19	-100.49	27.45
27	53	8.84	15.64	51.92

28	28	6.78	-107.10	27.20
29	34	2.00	-74.29	33.24
30	26	3.25	-108.43	25.29
31	34	11.47	-86.53	33.06
32	29	5.13	-68.96	27.85
33	26	5.02	-156.50	25.08
34	33	8.44	-169.04	31.57
35	17	2.09	-82.87	16.12
36	29	8.97	-96.11	28.16
37	21	6.03	-147.09	20.24
38	23	5.18	-68.19	21.54
39	25	7.36	-126.38	23.60
40	29	9.57	-100.12	28.44
41	36	6.11	-100.01	34.52
42	37	6.57	-105.94	36.40
43	35	2.67	-63.43	33.54
44	39	6.34	32.01	37.73
45	48	10.43	-30.96	46.64
46	60	7.56	-109.65	59.46
47	34	9.49	14.03	32.98
48	33	2.62	-90	32
49	41	1.31	-53.13	40
50	37	2.68	-96.34	36.22
51	37	1.77	-20.92	36.40
52	34	1.63	-45	32.52
53	32	2.1	-13.13	30.80
54	34	3.97	-72.12	32.57
55	43	2.49	-30.25	41.67

APPENDIX 3

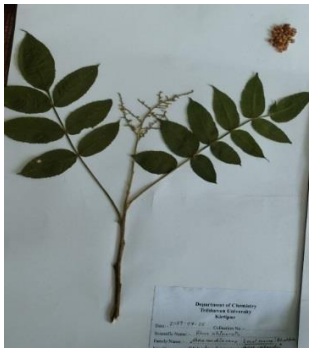

Herbarium of *Rhus chinensis*

Plant sample in powdered form

Extraction process

Phytochemical analysis

TLC plate

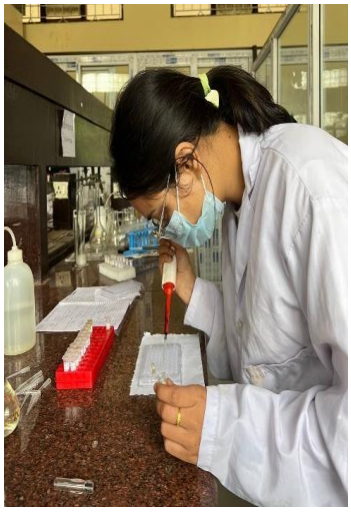

Loading sample in the 96 well plate

Microplate reader

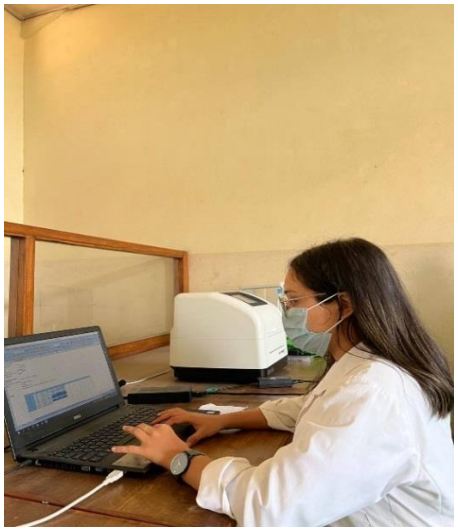

Analysis of data

Sample heated in magnetic stirrer at 60℃

Plant extract + silver nitrate in magnetic stirrer

UV- visible spectrophotometer

Sample mixture kept in cuvette

Analysis of absorption peak

Nano collection in centrifuge tube

Collected silver nanoparticles dried in a desiccator

Dried silver nanoparticles stored at 4℃ in a refrigerator